IR 79-1901

rec'd. 12/79

EA-6010-20
Dist. Category UC-90C

MATERIALS RESEARCH FOR THE CLEAN UTILIZATION OF COAL

QUARTERLY PROGRESS REPORT

April - June 1979

Samuel J. Schneider
Project Manager

Center for Materials Science
National Bureau of Standards
Washington, D.C. 20234

PREPARED FOR THE UNITED STATES
DEPARTMENT OF ENERGY

Under Contract No. EA-77-A-01-6010

"This report was prepared as an account of work sponsored by the United States Government. Neither the United States nor the United States Department of Energy, nor any of their employees, nor any of their contractors, subcontractors, or their employees, makes any warranty, express or implied, or assumes any legal liability or responsibility for the accuracy, completeness, or usefulness of any information, apparatus, product or process disclosed, or represents that its use would not infringe privately owned rights."

TABLE OF CONTENTS

		PAGE
I.	OBJECTIVE AND SCOPE OF WORK.	1
II.	SUMMARY OF PROGRESS TO DATE.	1
	Articles Published and Talks Presented	3
III.	DETAILED DESCRIPTION OF TECHNICAL PROGRESS	5
	1. Metal Corrosion.	5
	a. Pre-Cracked Fracture Text.	5
	2. Ceramic Deformation, Fracture and Erosion.	8
	3. Chemical Degradation of Ceramics	12
	a. Reactions and Transformations.	12
	b. Slag Characterization.	13
	c. Vaporization and Chemical Transport.	16
	4. Failure Prevention	24
	a. Failure Information Center	24
	b. Materials Properties Data Center	26
	5. Creep of MHD Refractories.	28
	6. Electrical Transport Mechanisms in Slag Associated with Electrochemical Degradation of Insulator and Electrode Materials.	29
	7. Corrosion of Downstream MHD Components	42

I. OBJECTIVE AND SCOPE OF WORK

Coal gasification and other conversion processes require the handling and containment of corrosive gases and liquids at high temperature and pressures, and also the handling of flowing coal particles in these environments. These severe environments cause materials failures which inhibit successful and long-time operation. The project entails investigations on the wear, corrosion, chemical and electrical degradation, fracture, and deformation processes which lead to the breakdown of metals and ceramics currently being utilized in test facilities and pilot plants. Studies will also be carried out on new candidate materials considered for improved performance. Special emphasis will be devoted to the development of test methods, especially short-time procedures, to evaluate the durability of materials in the severe environments. These methods will focus on wear, impact erosion, stress corrosion, strength, deformation, slow crack growth and chemical degradation. A system has been initiated to abstract and compile all significant operating incidents from coal conversion plants as well as materials property and performance information important to the design and operation of these plants. This program will provide a central information center where problems of common interest can be identified and analyzed to avoid unnecessary failures and lead to the selection of improved materials for coal conversion and utilization. Active consultation to DOE and associated contractors will be provided as requested.

II. SUMMARY OF PROGRESS TO DATE

Brief Summary

1. Metal Corrosion

a. Pre-cracked Fracture Test

Experimental verification of analysis for the change in stress-intensity ratio (K_T/K_o) with temperature was conducted for the tension-loaded DCB test fixture. The test specimen was 310 stainless steel, the loading fixture was 347 stainless steel, and the loading grip was Inconel 600. These tests demonstrated that the newly designed tension-loaded DCB testing method produces a nearly constant stress-intensity with increasing temperature, whereas, the currently used wedge-loaded/DCB testing method shows an unacceptably large decrease in stress-intensity with increase in temperature.

2. Ceramic Deformation, Fracture, and Erosion

Three studies were conducted this quarter in the apparatus for mechanical testing at elevated pressure and temperature. The first study was a continuation of some initial experiments that were begun last quarter. The goal of these initial experiments was to establish the satisfactory operation of the apparatus. The second study was conducted to calibrate the temperature profile inside of the environmental test chamber of the apparatus. With the successful completion of these studies, the third study was a series of controlled experiments to determine the flexural strength of

newly formulated batches of a high alumina (94%) refractory concrete in steam at elevated pressure and temperature. These studies are described in the text.

A similar series of controlled experiments will be undertaken next quarter on newly formulated batches of a low alumina (56%) refractory concrete. These specimens will be tested at nominally the same conditions that were used this quarter for the high alumina refractory. Following these experiments, time permitting, both of these refractory concretes will be tested in a simulated coal gasification environment at a nominal pressure of 1000 psia and a nominal temperature of 1010°C.

3. Chemical Degradation

a. Reactions and Transformations

In the simulated gasification environment, $\overline{CC}$ replaces hydrated calcium aluminate phases in high purity refractories. CC is stable to about 1100°C in dry CO_2 (500 psig), and to at least 975°C (1000 psig) in the dry gasification atmosphere. It dissociates near 625°C (1000 psig) when steam is added to the latter. AH dissociates at about 240°C (1000 psig).

b. Slag Characterization

Work continued on the measurement of viscosity of a slag having a composition of: SiO_2, 48%; Al_2O_3, 12.10%; Fe_2O_3, 12.00%; CaO, 14.90%; MgO, 8.00% and Na_2O, 4.7% (expressed in wt %). In 50% CO_2 and 50% steam at 97 psi the viscosity (log_{10}) was 1.46 at 1321°C, 1.72 at 1240°C, 1.73 at 1232°C and 1.98 at 1161°C. Measurements will be attempted at higher temperatures during the next quarter using a 60% Pt, 40% Rh heater.

c. Vaporization and Chemical Transport

Vapor transport data, in the form of alkali species partial pressures, have been obtained over a wide temperature (1500-1800 K) and pressure (10^{-6} - 1 atm) range for two different slag samples and in atmospheres containing the coal gas components of N_2, H_2O and H_2 (small concentration level only). As expected, the presence of H_2O or H_2 greatly increases the rate of K-release from the slag samples.

Following completion of the H_2O-slag system studies, the effects of higher concentrations of H_2 on alkali release will be determined. Complementary computer modeling of these experimental systems will also be attempted.

4. Failure Prevention

a. Failure Information Center

Ten additional reports of operating experiences and failure analysis were entered into the Center's data base. Over 170 information items were transmitted to plant operators and fossil energy contractors. Progress is continuing towards the completion of reports on corrosion and erosion failures.

A first draft of one section of the construction materials handbook has been completed. A feature article for the DOE Newsletter has been written and will be submitted for approval.

b. Materials Properties Data Center

During this quarter materials for a section of the Construction Materials Hankbook for Coal Gasification has been sent to DOE for approval, nine computer vendors' proposals for services have been received, reviewed, and technically evaluated, and material prepared for the MHD state-of-the-art review.

5. Creep of MHD Refractories

This task started during the quarter and the major efforts have been spent in modifying an existing high temperature creep apparatus to use for initial experiments in designing and ordering components for the complete 12-station creep apparatus.

6. Electrical Transport Mechanisms in Slag Associated with Electrochemical Degradation of Insulator and Electrode Materials

Yttrium chromite doped with Ca or Mg appears to be a viable electrode material for a hot or semi-hot wall MHD generator. High density material has been made and the electrical conductivity measured over the temperature range from 25 to 1650°C. Preliminary measurements of its electrochemical corrosion resistance show that anode degradation is much less than that of the cathode.

The electrical conductivity of Eastern coal slag (Bow NH) without added potassium has been measured under carefully controlled conditions. The low temperature conductivity, i.e., conductivity below 900°C falls on two definite curves depending on the temperature from which the sample was quenched. Fe_3O_4 appears to be the conducting medium in the high conductivity curve for samples quenched from above 1375°C. Samples quenched from below this temperature have anorthite ($CaAl_2Si_2O_8$) as the only detectable crystalline phase in a glassy matrix and have low conductivities.

7. Corrosion of Downstream MHD Components

Extensive changes were made to the extant burners rig, to provide more control over test variables and to extend the testing capability to a longer term (> 100 hours). Specimen size and preparation details were worked out as well as the technique for making oxygen partial pressure measurements in the hot gas zone in the immediate vicinity of the specimen. Plans for the coming quarter include the start of four hour and one-hundred hour tests on 304 and 316 stainless steel.

Articles Published and Talks Present

"Mechanical Property Testing of Refractory Concretes at High Pressure and Temperature", E. R. Fuller, Jr., S. M. Wiederhorn, and D. E. Roberts, at 81st Annual Meeting of American Ceramic Society, Cincinnati, Ohio, April 29 - May 2, 1979.

F. A. Mauer and C. R. Robbins, "X-ray Powder Diffraction Measurements in Reactive Atmospheres at 1000°C and 7 MPa (1000 psig)," in Advances in X-ray Analysis, vol. 22 (1979).

Preparation and Properties of Yttrium Chromite Ceramics, T. Negas, W. Hosler, National Bureau of Standards and L. Dominques, Trans-Tech, Inc., 4th International CIMTEC Energy and Ceramic Conference, Faenza, Italy, May 28-31, 1979.

II. DETAILED DESCRIPTION OF TECHNICAL PROGRESS

1. Metal Corrosion

a. Pre-cracked Fracture Test (J. H. Smith and G. E. Hicho, 562)

Progress: Tests to experimentally verify the analysis for the change in stress-intensity ratio (K_T/K_o) with temperature for the tension-loaded DCB specimen were continued. The redesigned loading fixture for stressing the tension-loaded DCB specimen that was described in reference 1 was used. The loading fixture was made of type 347 stainless steel, the loading grips were made of Inconel 600 and the specimen was made of type 310 stainless steel.

The experimental verification of the predicted change in stress-intensity ratio, (K_T/K_o) with temperature requires that the displacement at the specimen crack line, V_T, be measured as a function of temperature. Previous attempts to measure this change in crack line displacement, V_T, as a function of temperature have proven to be insufficiently accurate to verify the analytical equation for the change in stress-intensity ratio, (K_T/K_o) with temperature. Therefore, an experimental apparatus was designed and set up to determine the crack-line displacement, V_T, changes with a linear-voltage displacement transducer (LVDT). The results of these tests are shown in Figure 1. These tests showed that the stress-intensity ratio, (K_T/K_o), for the 310 specimen in the tension-loaded DCB fixture increases slightly (less than 7% on heating to 275°C. That is, this particular specimen-loading fixture is nearly thermally compensated so as to produce a nearly constant stress-intensity with temperature. In contrast, a conventional wedge-loaded DCB specimen decreases by over 10% as the temperature is increased from 0°C to 275°C as shown in Figure 1. The analysis developed in reference 2 predicts that the K_T/K_o ratio will increase by about 13% as the temperature is increased to 275°C, as shown in Figure 1. Therefore, the present experiments show that the tension-loaded DCB specimen maintains nearly constant stress-intensity factor with increasing temperature. However, the predicted change in stress-intensity ratio (K_T/K_o) given in reference 2 may not be accurate and will require modification to agree with the present experimental results.

Plans: Additional experimental tests will be conducted to determine the change in stress-intensity ratio (K_T/K_o) with temperature. Refinements will be made in the measurement of crack-line displacement and temperature in these experiments. The verification experiments will be extended to higher temperatures. Attempts will be made to conduct tests up to 600°C but these may be limited to a lower temperature if substantial creep occurs in the specimen or loading fixture. The analysis for predicting the change in stress-intensity ratio (K_B/K_o) with temperature will be modified to agree with the results of the experimental verification tests.

Initial laboratory testing of specimens of 310 and 304 stainless steel and of Incoloy 800 which have been prepared will be initiated. Preparation of a summary report of results obtained to date will be initiated.

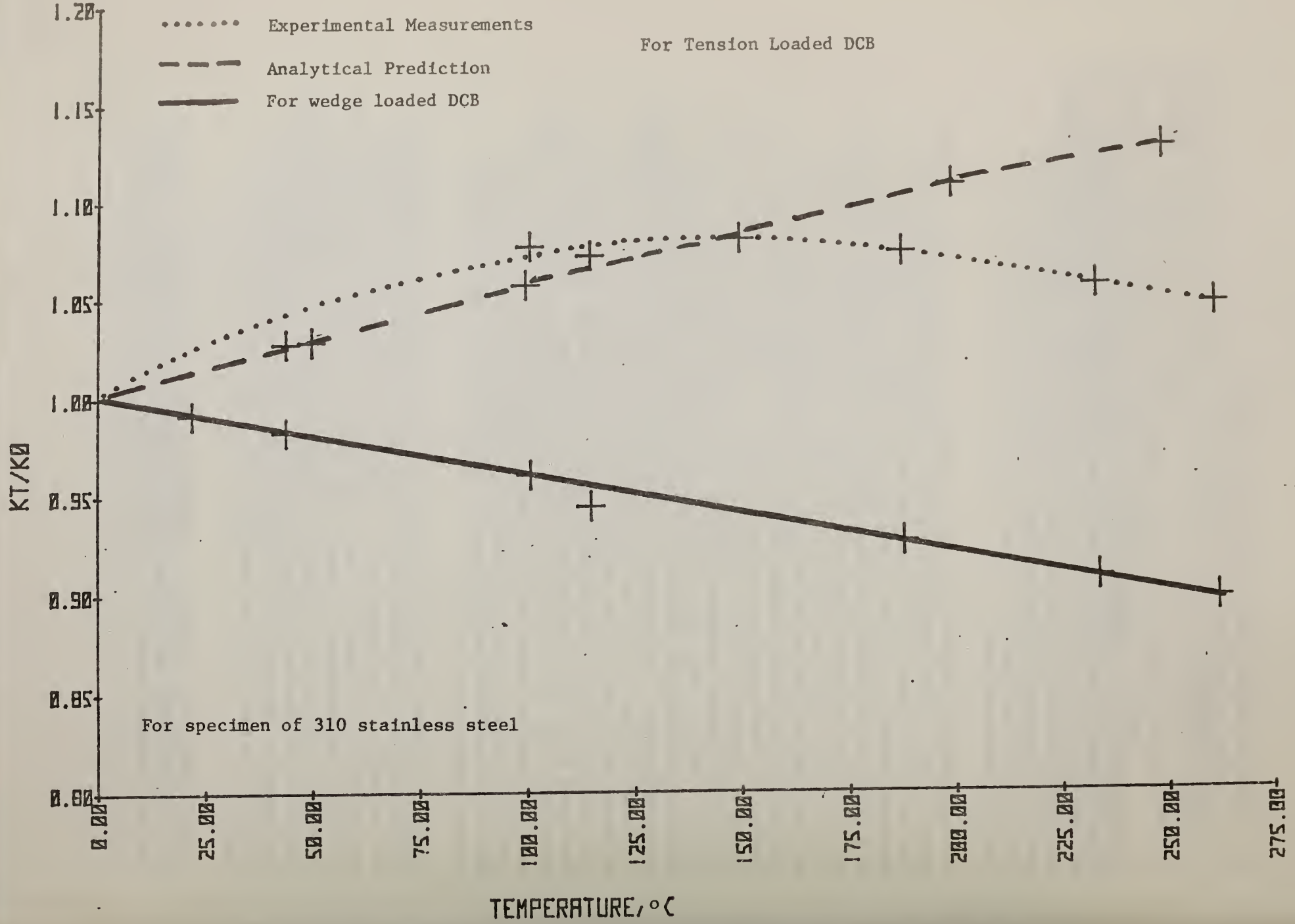

Effect of Temperature on Stress-Intensity

References

1. NBS Quarterly Report to DOE: January 1, to March 31, 1979 "Materials Research for Clean Utilization of Coal." EA-6010-20, Dist. Cat. UC-90C.

2. NBS Quarterly Report to DOE: January 1 to March 31, 1978 "Materials Research for Clean Utilization of Coal." EA-6010-20, Dist. Cat. UC-90C

2. Ceramic Deformation, Fracture, and Erosion (E. R. Fuller, Jr., S. M. Wiederhorn, D. E. Roberts, and L. Chuck, 562)

Progress: Three studies were conducted this quarter in the apparatus for mechanical testing at elevated pressure and temperature. The first study was a continuation of some initial experiments that were begun last quarter. The goal of these initial experiments was to establish the satisfactory operation of the apparatus. The second study was conducted to calibrate the temperature profile inside of the environmental test chamber of the apparatus. With the successful completion of these studies, the third study was a series of controlled experiments to determine the flexural strength of newly formulated batches of a high alumina (94%) refractory concrete in steam at elevated pressure and temperature. These studies are described in detail below.

To establish the elevated pressure and temperature operation of the mechanical testing apparatus, two additional experiments were conducted at the beginning of the quarter. In the first experiment, which was ongoing from last quarter, specimens of a high-alumina refractory concrete were exposed to steam at a pressure of 4.55 MPa (660 psia) and at a temperature of 410°C for 110 hours. The specimens were then broken at the elevated pressure-temperature conditions. The strength of these specimens was only slightly weaker than the strength of untreated, or control, specimens. See Table 1. In the second experiment, high-alumina refractory specimens were tested after exposure to steam at a pressure of 4.86 MPa (705 psia) and a temperature of 510°C for 90 hours. The strength of these specimens was similar to that of the specimens exposed at 410°C. Results of both of these initial experiments are tabulated in Table 1. Also listed are the crystalline mineral phases that were determined for each specimen after the exposure and strength measurement at elevated pressure and temperature.

Following these initial experiments, a short study was undertaken to establish the temperature profile inside the environmental test chamber for various nominal temperatures and pressures. To measure the temperature profile, a modified internal fixture was devised to replace the upper loading assembly. This fixture consisted of a blank flange through which four high-pressure thermocouple "feed-thrus" was made. The specimen loading fixture was attached to the inside of this flange, and refractory concrete specimens were positioned on the first and last loading stations of the fixture. Each of these specimens had two sheathed thermocouples embedded inside the refractory; one in a hole at the center of the specimen and the other in a hole near one end of the specimen. Results showed that at thermal equilibrium a slight temperature gradient could exist along the length of each specimen (approximately 3 to 5°C, maximum, with the direction of the gradient being dependent on the specimen position) and that the specimen temperature was approximately 25°C different than the heater-element temperature. Another important result of these experiments was that a mode of heating was established that allows the specimens to increase in temperature and pressure along the saturated vapor cure. Previous experiments have shown that these heating conditions help establish crystalline phase equilibrium more rapidly than when the specimens were heated under drier conditions.

Having determined the temperature conditions at the specimens for various furnace settings, a series of experiments were conducted on newly formulated batches of a high-alumina (94%) refractory concrete. These experiments consisted of a measurement of the flexural strength at pressure and temperature following a 100 hour exposure in high-pressure steam at temperatures of nominally 360°C, 660°C, and 1010°C. To complement these strength measurements at temperature and pressure, additional refractory specimens were exposed simultaneously with the strength specimens. These additional specimens were then tested at room temperature and atmospheric pressure after the elevated pressure-temperature exposure. Initial results from these experiments are illustrated in Figure 1 where the fracture loads are plotted for specimens broken at various exposure temperatures and for similar specimens broken after the exposure. The greatest discrepancy in these strength measurements was observed for 1010°C experiment. Under these exposure conditions, the strength measured at temperature and pressure was approximately 2 to 3 times greater that the strength measured after exposure. X-ray diffraction analysis and examination of the specimens with scanning electron microscopy is currently in progress.

Plans: A similar series of controlled experiments will be undertaken next quarter on newly formulated batches of a low alumina (56%) refractory concrete. These specimens will be tested at nominally the same conditions that were used this quarter for the high alumina refractory. Following these experiments, time permitting, both of these refractory concretes will be tested in a simulated coal gasification environment at a nominal pressure of 1000 psia and a nominal temperature of 1010°C.

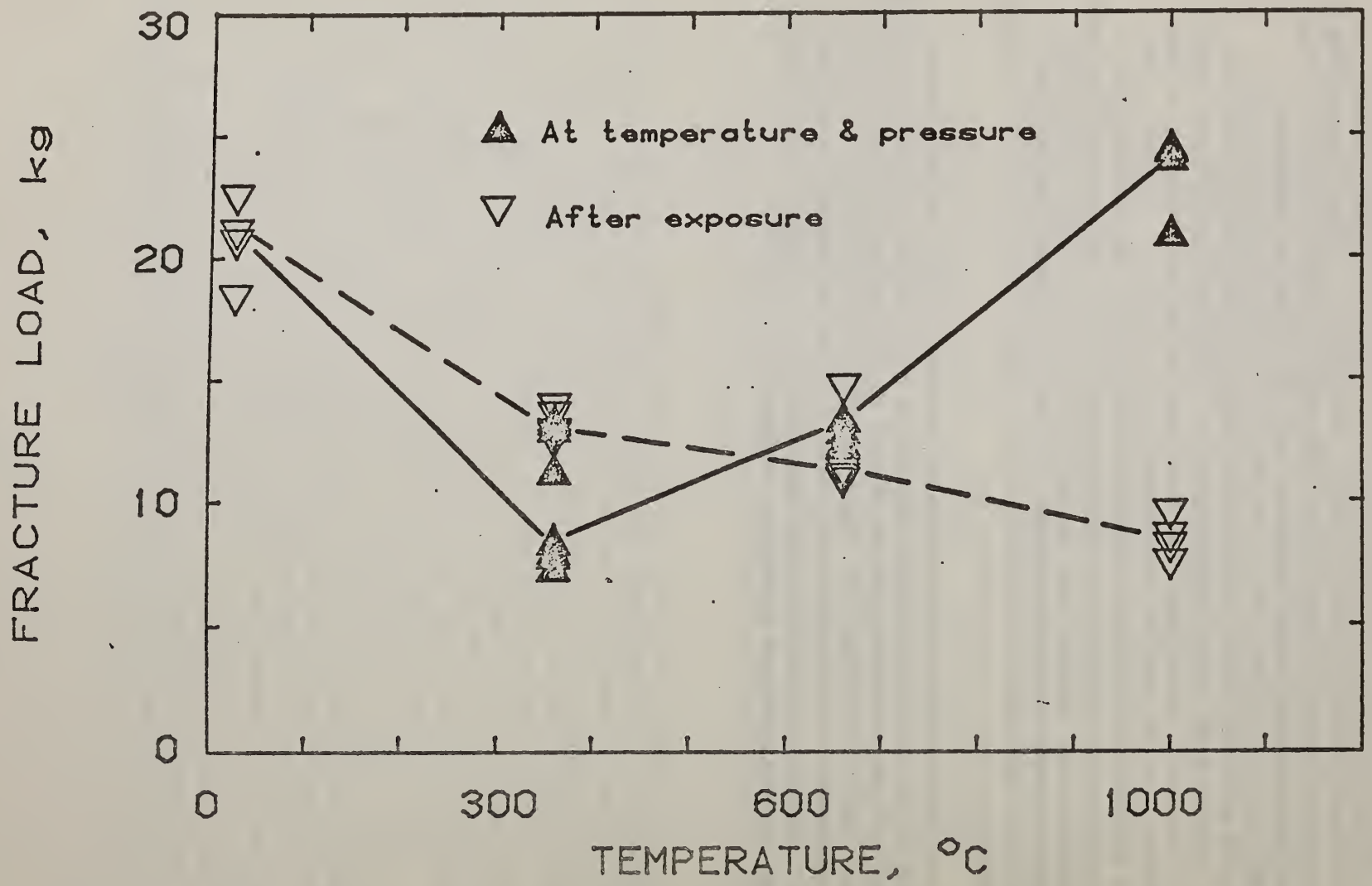

Figure 1. Fracture load of a high-alumina refractory concrete as measured both at temperature and pressure in steam (up triangles and solid line), and after exposure (down triangles and dashed line).

Table 1. *In-Situ* Strength of a high-alumina refractory concrete in elevated pressure-temperature steam.

Exposure Condition	Median Strength	Mineral Phases *
Control (dried at 110°C and fired at 1010°C)	14.8 MPa 2,150 psi	α-alumina, $CaO \cdot Al_2O_3$, and $CaO \cdot Al_2O_3$
110 h at 410°C and 4.55 MPa	10.9 ± 0.3 MPa 1,590 ± 50 psi	α-alumina, and $CaO \cdot 2Al_2O_3$
90 h at 510°C and 4.86 MPa	11.2 ± 1.2 MPa 1,630 ± 170 psi	α-alumina, $CaO \cdot 2Al_2O_3$, and $CaO \cdot Al_2O_3$

* Mineral phases were determined at room conditions after the elevated pressure-temperature exposure and strength measurement.

3. Chemical Degradation of Ceramics

a. Reactions and Transformations (F. A. Mauer and C. R. Robbins, 565)

Progress: A test bar of unfired calcium aluminate binder was exposed to the simulated gasification environment in a series of three experiments. Chemical reactions were monitored by the *in situ* x-ray method as temperatures and pressures were varied.

Formation of hydrated calcium aluminates was suppressed by the presence of CO_2 in the environment. The phase assemblage at 270°C/1000 psig* was α-A, $\bar{C}A$, AH and $C\bar{C}$. With increasing temperature, AH started to dissociate at about 240°C/1000 psig. Small amounts of this compound persisted to ∿ 100°C above the dissociation temperature, as previously observed in this work. At near 625°C/1000 psi, $C\bar{C}$ began dissociating, and this reaction was accompanied by the formation of CA_2. Growth of bonding phase CA_2 was moderate at 800°C, but rapid in the temperature interval 900-1000°C (1000 psig).

In the simulated gasification environment, $C\bar{C}$ replaces hydrated calcium aluminates as the bonding phase coexisting with AH or α-A. *In Situ* experiments using a test bar of $C\bar{C}$ in dry CO_2 (500 psig) show that $C\bar{C}$ is stable to about 1100°C. In the dry gasification atmosphere it appears stable at 975°C/1000 psig. With the addition of steam to this environment, the dissociation temperature of $C\bar{C}$ is lowered by about 400°C.

An experiment is in progress involving exposure of a test bar of calcium aluminate binder to steam in order to delimit regions of temperature in which the various phases encountered are stable. Forty energy dispersive x-ray patterns have been recorded.

Phase analysis of refractory specimens from a modulus of rupture study were made by conventional x-ray methods for Task 2. Results will be given under that section.

Plans: Test bars of A-56 and CAS_2 will be studied in the simulated gasification atmosphere.

* In SI units, 1 MPa = 145 psia.

b. Slag Characterization (W. S. Brower, J. L. Waring, and D. H. Blackburn, 565)

Progress: Work was continued on the measurement of viscosity of a slag with the following composition: SiO_2, 48%; Al_2O_3, 12.10%; Fe_2O_3, 12.00% CaO, 14.90%, MgO, 8.00%, Na_2O, 4.7% (expressed in wt percent). As reported previously, an attempt was made to determine the viscosity of this material in CO_2 and steam. Ten psi of CO_2 pressure was added to 55 psi of steam in the viscometer. Earlier the material was heated briefly in CO_2 and some crystals had apparently formed on the surface of the melt. When the bob was introduced into the melt it apparently contacted the crystalline mass, moved off center and was effectively welded to the side of the crucible. This ruined the crucible containing the melt and the suspension. The old crucible was unwelded from the platinum heater with a hammer and chisel and the heater was then reshaped. A new torsion wire was fabricated and calibrated. This wire was added to a new thermocouple and to a bob to form the suspension.

Using a new crucible and a new batch of the quenched glass slag, the viscosity was measured in 50% CO_2 and 50% steam at 97 psi total pressure. At 1321°C, 1240°C, 1232°C, and 1161°C, the viscosity was found to be log η = 1.46, 1.72, 1.73, 1.98 respectively. The results are related to previous data as shown in Figure 1.

At this point it was decided not to continue viscosity measurement in mixed gaseous environment but to increase the temperature of viscosity measurements with the existing heater in steam until burn out occurred. When this occurs the heater will then be replaced with 60%Pt-40%Rh in hopes of obtaining higher temperatures. Therefore, the melt previously heated in CO_2 and steam was heated to a melt temperature of 1386°C in an attempt to remove the CO_2 and any residual crystallites. The viscosity bob was re-introduced into the melt and steam was generated up to 75 psi. When the crucible was rotated no deflection was indicated on the magnetic position detector. The run was again aborted; the crucible which lifted from the pedestal and welded to the heater was again removed from the heater with a hammer and chisel and the entire process described previously was duplicated.

In all the earlier experiments each crucible had a large bottom fin welded to the bottom. This crucible was potted to a ceramic pedestal and fired to 1400°C. The procedure took about a week. For the present experiments this process was shortened to save time by reducing the size of the bottom fin and attaching the crucible to the pedestal with "alumina cement." The "alumina cement" was fired in place during the course of the run. However, the presence of high pressure steam apparently did not allow the maturing of the cement. In the current experimental setup, the size of the bottom fin has again been increased, and the original groove in the ceramic pedestal cleared with a diamond saw. The crucible and pedestal are held together with a lower temperature "green-cast" cement. This experimental procedure should now be sufficient to hold the crucible to the pedestal during rotation.

While attempting to make the final run at temperatures higher than 1380°C, a malfunction developed in the temperature controller. When the system was taken apart once again, a heavy oxide coating and remnants of residual arc melting were seen on the contacts of the copper feed through which supply power goes to the platinum heater.

Plans: Rebuild the apparatus and gain as much viscosity information as possible with the existing heater until burn out occurs. Then attempt to extend the temperature in steam by using a new heater fabricated from 60%Pt-40%Rh.

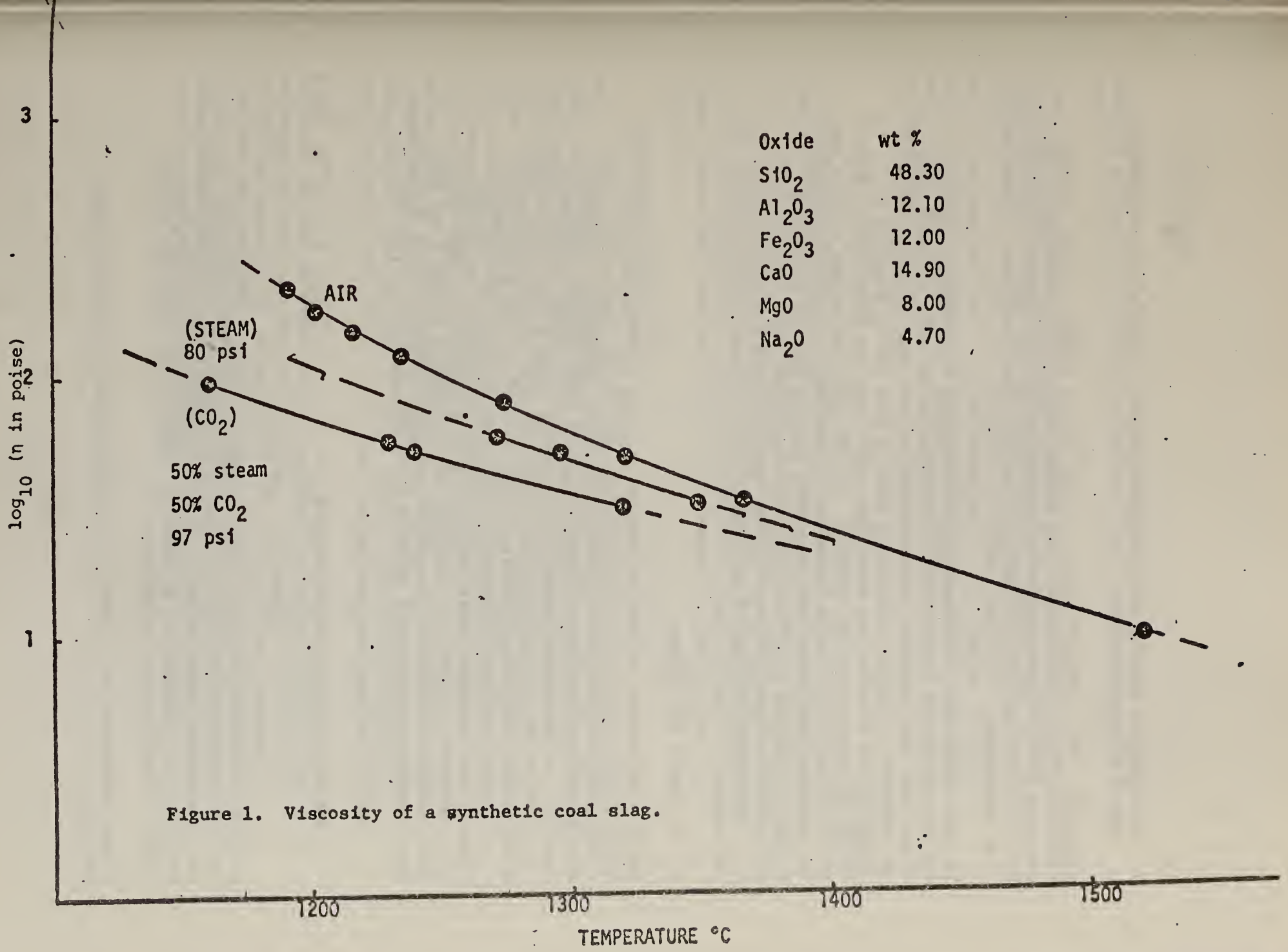

Figure 1. Viscosity of a synthetic coal slag.

c. Vaporization and Chemical Transport (J. W. H. Hastie, D. W. Bonnell, and E. R. Plante, 561)

Progress: Vapor transport data, in the form of alkali species partial pressures, have been obtained over a wide temperature (1500-1800 K) and pressure (10^{-6} - 1 atm) range for two different slag samples. The effect of H_2O vapor and small H_2 concentrations on the alkali transport process was also determined.

We have found that it is necessary to establish the chemical reactions and characteristic mass spectral fragmentation patterns for each individual coal gas component before proceeding with complex multicomponent gas mixtures. Without such a data base it will not be possible to interpret the observations made with actual coal gas atmospheres, even though such data could be obtained. Of the two slag systems studies one is the so-called K_1 system (based on Illinois No. 6 coal), discussed in the previous (Jan.-Mar. 1979) Quarterly Report, and the other is a synthetic "Western type" coal slag of composition (wt%), SiO_2 (47.3), Al_2O_3 (11.1), Fe_2O_3 (12), CaO (13.9), MgO (7.0) and K_2O (8.7) denoted as K_2. Complementary computer modeling of these systems has also been initiated.

1. K_1 slag + H_2O System:

The K_1 slag system, of initial compositon Al_2O_3 (12.06), CaO (3.8), Cr_2O_3 (1.3), Fe_2O_3 (14.25), K_2O (19.54), MgO (1.03), Na_2O (0.47), SO_3 (0.21), SiO_2 (46.82), and TiO_2 (0.52) wt%, has previously been characterized by vaporization in a N_2 atmosphere (see previous Quarterly report). In the present study, the effect of added H_2O on the release of alkali to the gas phase was monitored with the transpiration mass spectrometer (TMS) from 1280-1419 °C and 10^{-3} - 10^{-1} atm H_2O vapor in $\sim$ 0.5 atm N_2. Typical data are given in Figures 1 and 2. Note in Figure 1 the relatively small dependence of K-pressure on temperature at a constant H_2O pressure. However, as is shown in Figure 2, at constant temperature, the K-pressure is strongly dependent on the H_2O-pressure. The following reactions are believed to be responsible for this effect.

$$K_2O\ (\ell)\ \text{(in slag)} + H_2O = 2KOH \qquad (1)$$

$$K_2O\ (\ell)\ \text{(in slag)} + H_2 = 2K + H_2O \qquad (2)$$

$$H_2O = H_2 + 1/2\ O_2. \qquad (3)$$

We believe that reaction (2) is the predominant mechanism for H_2O-induced alkali release under the conditions pertaining to Figure 2 and that the thermal dissociation of water (reaction (3)) provides the necessary H_2. However, as is shown in Figure 2, the reactions do not appear to have attained equilibrium.

Future experiments with added H_2 gas are planned to test this interpretation.

2. K_2 slag System

A lower melting, more basic, (as compared with the K_1 sample) synthetic slag was prepared for studies analogous to those performed for the K_1 system.

Under free vaporization (KMS) or N_2-atmosphere (TMS) conditions the predominant vapor species in this system are K and O_2; pressures are shown in Figure 3. The initial excess of O_2 present in this slag is believed to result from the preparation procedure where melting and pouring in room air led to oxygen absorption by the sample. Pressure bursts of K and O_2 were noted in the initial phase of the TMS experiments, e.g., at 1500 K in Figure 3 suggesting that trapped gas was released from the slag.

3. K_2 slag + H_2O system

The appreciable effect of H_2O vapor on the release of K from the K_2 slag is demonstrated in Figure 4. The data are consistent with reaction (2) as the primary process leading to the enhanced release of alkali. Also, as the data agree with the thermodynamic pressure dependence (slope 0.5 for curve of Figure 4), the system appears to be at equilibrium. In addition to this process, reaction (1) was also observed, but to a much lesser degree than reaction (2), by the presence of KOH as shown in Figure 5.

4. Thermodynamic modeling

Previous attempts at modeling complex multicomponent systems, including slags, have either assumed ideal solution behavior or an ideal mixing of hypothetical complex species. However, it is well known, and our experimental data confirm this, that slags form highly non-ideal solutions. Accordingly, we have applied, for the first time, a non-ideal solution multicomponent equilibria computer program to a slag system. The program known as SOLGASMIX is based on the development by Eriksson [(G. Eriksson, Chemica Scripta, 8, 100 (1975)]. As a test case we have taken the K_2 slag system with a atm H_2 present. Typical data are given in Table 1 where the effect of non-ideal solution behavior is clearly demonstrated. Also at 1500 K, the K species is much more significant than KOH; 87% of the alkali is released as K under these conditions.

Plans: Following completion of the H_2O slag interaction studies, moderate levels of H_2 will be added to the atmosphere and vapor transport measurements made on the same slag systems. The amount of H_2 added will be determined mainly by the durability of the Pt reactor components to the reducing atmosphere. Using a computer based non-ideal solution model, the experimentally observed effect of H_2 and H_2O on alkali vapor transport will be analyzed thermodynamically and the results extended to the pressure and temperature regime of slagging coal gasifiers.

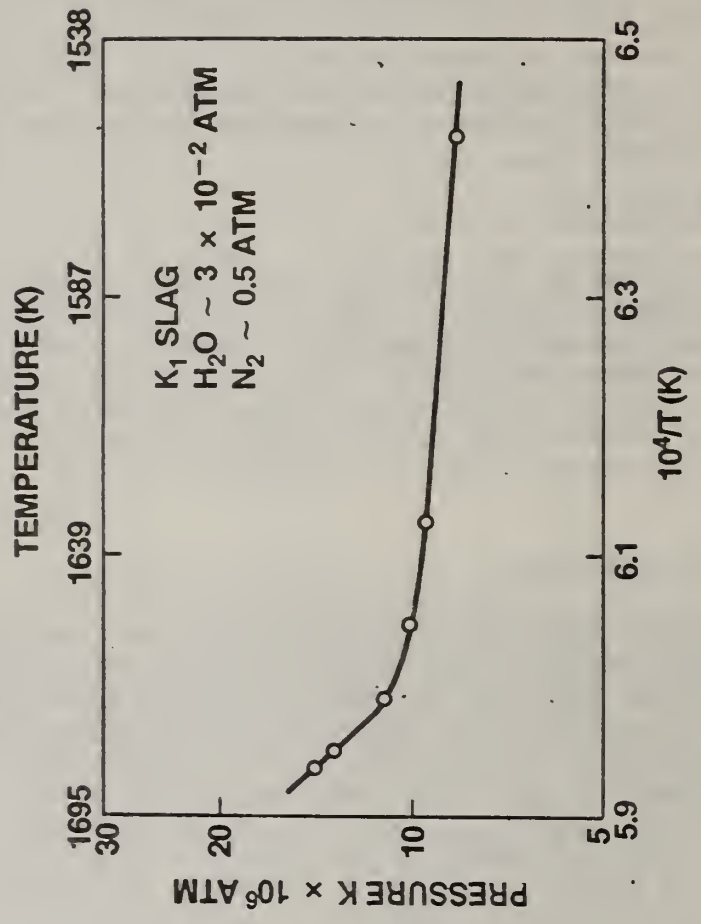

Figure 1. Dependence of K-pressure on temperature in the presence of H_2O ($\sim 3 \times 10^{-2}$ atm) and N_2 (0.5 atm) for the K_1 slag. The following ionization cross sections were used to convert intensities to partial pressures: N_2 (1.46), K (7.5), H_2O (3.2).

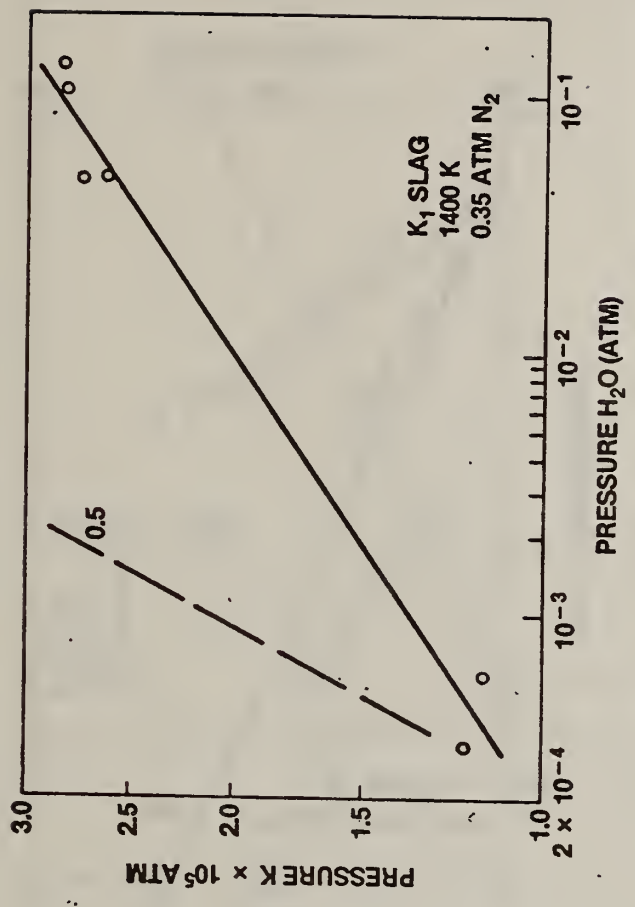

Figure 2. Dependence of K-pressure on H_2O content in N_2 (0.35 atm) at 1400 K for the K_1 slag. The dashed curve of slope 0.5 represents the theoretical (thermodynamic equilibrium) dependence for reactions (1) and (2) (see text). At 1400 K, the K_1 slag is a solid.

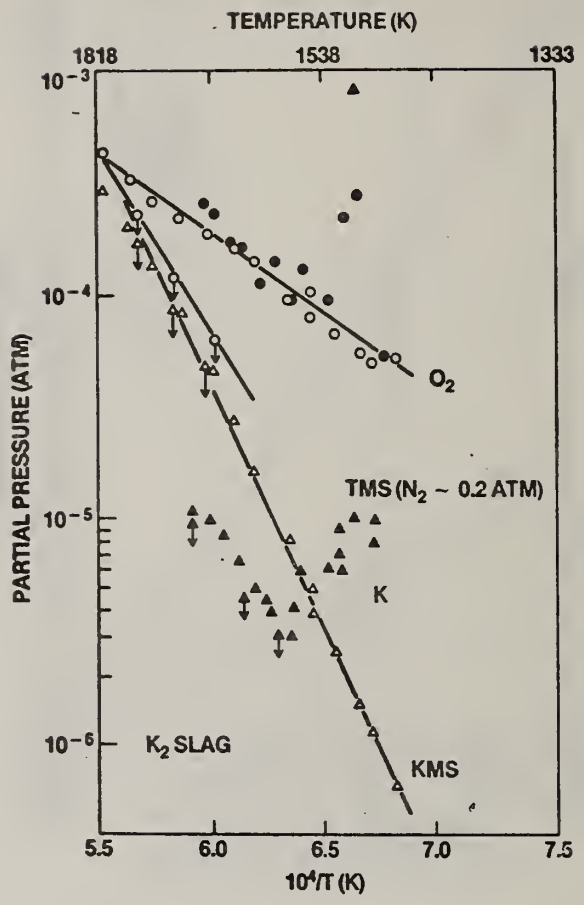

Figure 3. Vaporization of K and O_2 from the K_2 slag, expressed as log P vs 1/T plots: open circles - O_2 (KMS), closed circles - O_2 (KMS), closed circles - O_2 (TMS), open triangles K (KMS), closed triangles K (TMS). Chronological order of data taken with increasing temperature except for arrowed data points where the temperature was decreasing.

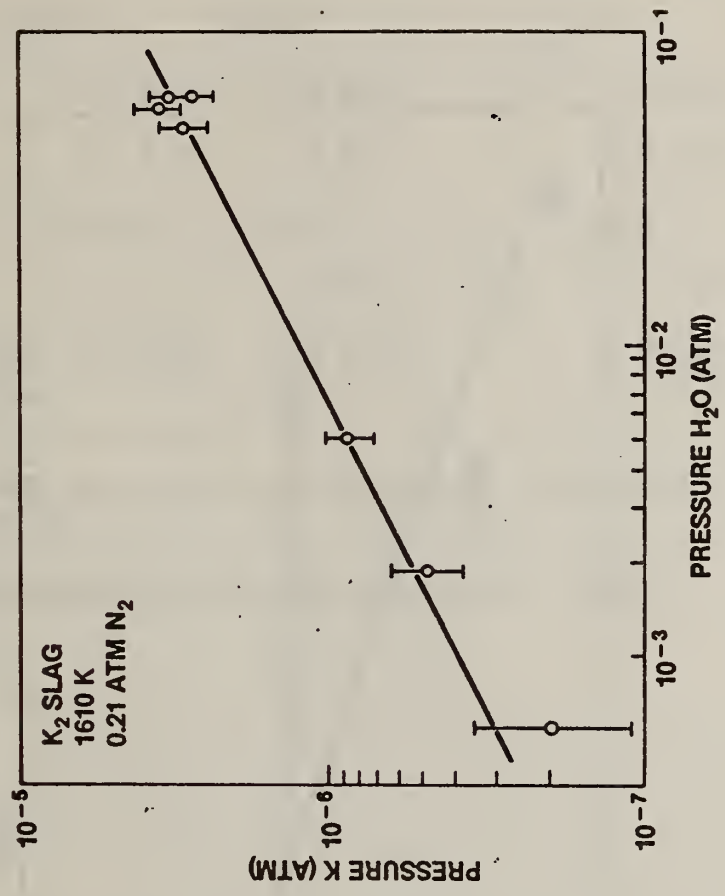

Figure 4. Dependence of K-pressure on H_2O-Pressure at contant temperature for the K_2 slag (TMS data). The curve of slope 0.5 represents the theoretical pressure dependence for reaction (2) (see text).

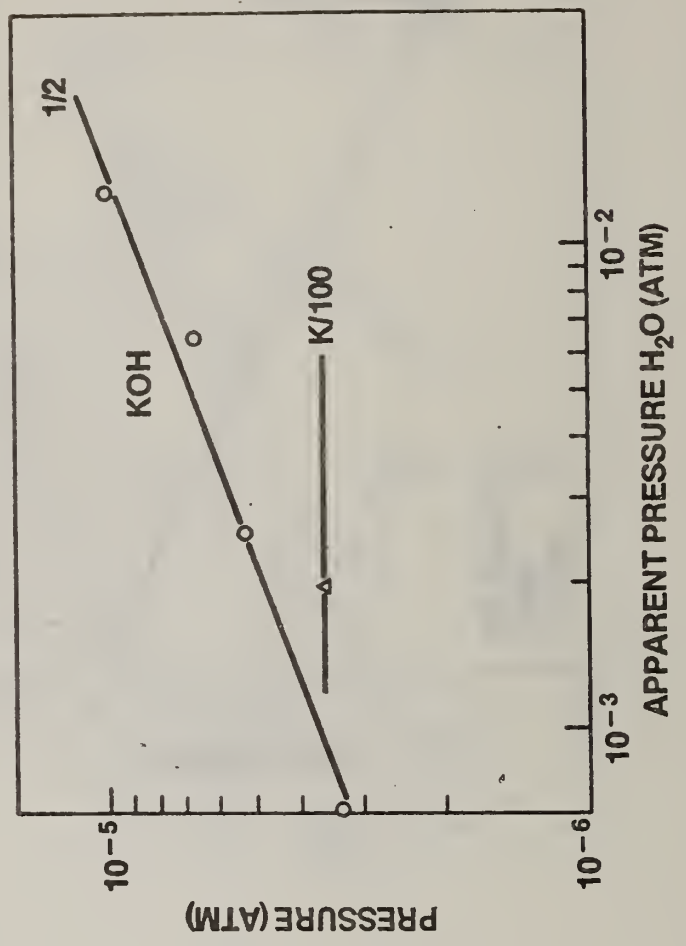

Figure 5. Dependence of KOH-pressure on H_2O apparent pressure at constant temperature for the K_2 slag (KMS data). The curve of slope 0.5 represents the theoretical pressure dependence for reaction (1).

Table 1

EXAMPLE OF THERMODYNAMIC MODEL OUTPUT[a]

	Ideal Solution		Non-ideal Solution[b]	
P(atm) T(K)	1000	1500	1000	1500
K	6.7 E-3	1.8 E-2	3.3 E-8	4.6 E-6
KOH	1.4 E-2	3.3 E-3	8.2 E-8	6.7 E-7
H_2	0.96	0.95	0.97	0.97
H_2O	2.3 E-2	3.4 E-2	2.7 E-2	2.7 E-2
O_2	4.2 E-24	4.5 E-15	5.7 E-24	2.7 E-15

[a] System K_2 slag wt%; SiO_2 (47.3), Al_2O_3 (11.1), Fe_2O_3 (12), CaO (13.9) MgO (7.0), K_2O (8.7).

[b] Activity K_2O experimental input (K_2O + SiO_2 data used).

4. Failure Prevention

a. Failure Information Center (R. C. Dobbyn, W. A. Willard, 562 and W. S. Brower, 565)

Progress: During the quarter the Failure Information Center received ten reports of operational experiences and materials and components failures in coal conversion pilot plants and process development units. To date, the percent contribution of failure incidents contained in the data base is shown in Table I.

These reports have been classified and evaluated for technical completeness and accuracy. Detailed summaries of this information have been entered into the Center's computerized data bank.

The Center continued to aid Battelle-Columbus in their preparation of the DOE Materials and Components Newsletter. Two updated statistical summaries of operating experiences were supplied to Battelle for inclusion in the DOE Newsletter feature on failures.

The Failure Information Center answered twelve requests for information during this quarter. The response to these inquiries resulted in the dissemination of 120 abstracts and 51 hard copy reports. In addition, three visitors received detailed briefings on the Center's present and planned activities.

Work is continuing on the reformatting of the data base and should be completed during the next quarter. In addition, the Failure Information Center's work with the Materials Properties Data Center on the Performance and Properties Handbook of Construction Materials for Coal Gasification is continuing. A draft of the first section of the handbook has been completed (see section 4b).

Progress is continuing in the analysis of reported corrosion and erosion failures. A draft report on corrosion problems is being prepared and the analysis of erosive wear failures is continuing.

A feature article for the DOE Materials and Components Newsletter relating the performance of the CO_2 Acceptor Pilot Plant gasifier refractory lining was completed and will be submitted to the DOE staff for approval.

The Morgantown Energy Technology Center was visited and additional information on solids valves was obtained for inclusion in the construction materials handbook.

Plans: Plans for the next quarter include: completion of the draft report on corrosion failures in the coal conversion industry; completion of reformatting of failure information data base; visits to selected pilot plants; continuation of work on coal gasification construction materials handbook.

Table I

Failure Incidents in the Coal Conversion Industry

Process	No. of Incidents	Percent
BIGAS	16	3.6
BMI	35	8.0
CARBONATE	5	1.1
CLEAN COKE	26	5.9
CO_2	52	11.8
CRESAP	20	4.5
EXXON	3	0.7
GFETC	2	0.5
HYGAS	45	10.2
LETC	3	0.7
LIGNITE	18	4.1
METC	13	3.0
MISC.	15	3.4
PETC	2	0.5
SRC	22	5.0
SRC-W	16	3.6
SYNTHANE	115	26.1
SYNTHOIL	2	0.5
WESTINGHOUSE	30	6.8

440 = Total Number of Incidents

b. Materials Properties Data Center (H. M. Ondik, T. A. Hahn, and A. Perloff, 565, I. J. Feinberg, 562)

Progress: A section on solids valves for the Construction Materials Handbook for Coal Gasification has been sent to the DOE project monitor for comments and approval of style, format, and content. The materials sent to the monitor corresponds to the items marked with asterisks in the following partial outline of the Handbook--

Section A. Construction Considerations and Performance Data

1. Coal Handling and Preparation Equipment
.
.
.
.

11. Valves
    11.3 Solids Valves
        11.3.1 Operating Requirements***
        11.3.2 Performance Data
            11.3.2.1 Materials Evaluation Tests***
            11.3.2.2 Component Test and Development***
            11.3.2.3 Plant Experience***
        11.3.3 Candidate Materials

The information contained in the "Materials Evaluation Tests" portion includes the results of testing of samples of materials considered for possible use as trim components in valves. The testing included resistance to erosion and abrasion of a large variety of materials and the effect of thermal shock and temperature cycling on the properties of some refractories. The "Component Test and Development" portion currently contains the results of seat leakage tests performed on actual valves mounted on a test stand. The "Plant Experience" portion includes in-service performance information gleaned from the NBS-DOE Failure Information Data Bank. The "Candidate Materials" section will not be written until further information has been gathered and entered into the "Performance Data" section so that the most reasonable and best possible selections based on all available data can be made for the possible candidate materials.

Nine proposals for computer vendors' services were received from vendors in mid-May. About seven full days of the Center staff's time were required for the technical evaluation and review of the proposals. Four of the proposals were rejected as not meeting the mandatory requirements as stated in our request for proposals. The other five were acceptable with the proviso that the vendors clarify or expand various statements

in the proposals. Since the vendors of the four rejected proposals may appeal our evaluation and since it is possible that not all of the five partially acceptable proposals will be clarified to our satisfaction, we cannot yet know how many of the vendors' proposals will be eligible for benchmark testing. As yet, no responses have been received from any of the vendors.

The normal operations of the Data Center continue with regard to handling of materials research contractors' reports and data, and work on the Hankbook and the state-of-the-art review of MHD materials.

Plans: It is expected that during the coming quarter benchmark testing will be conducted to determine which computer vendor's services will be contracted, normal data operations of the Center will continue, further sections of the Construction Materials Handbook for Coal Gasification will be prepared, and the MHD materials state-of-the-art review will be completed.

5. Creep of MHD Refractories (N. J. Tighe, S. M. Wiederhorn and C. McDaniel, 562)

Progress: An existing deadweight loading apparatus was modified to measure deflection of a specimen with a linear variable differential transducer. The creep testing apparatus has SiC loading rams and is equipped with a furnace capable of operation up to 1650°C.

Samples of the refractories designated X-317* and RFG* were obtained from from Fluidyne and Montana State University. These samples were cores taken from the refractory bricks used in the air-preheater test rigs. Because these materials react with the SiC rams it was necessary to find a non-reactive materials for separating pads. A series of tests showed that alumina was most compatible with both rod and specimen. However, some of the alumina compositions showed considerable creep at 1600°C and a design modification must be made.

The first modification will be to make longer specimens with a reduced cross-section. With this type of specimen the portion having the reduced cross-section will be in the hot zone and the ends will extend beyond the hot zone where the pads do not exhibit creep.

A few preliminary creep runs were made with the Corhart X-317 with $\sim$ .08" (2 mm) thick alumina pads. The specimens were 3/4" in diameter and 1" long. Specimens were weighed and measured before and after test runs at 1400°C, 1500°C and 1600°C. Specimens were held at: 1400°C for 68 hr. at 31 psi; 1500°C for 74 hr at 31-56 psi; and 1600°C for 86 hr at 31-124 psi. Although some sintering occurred between the alumina and the X-317, there was no evidence for creep in the X-317.

Furnaces and other components have been ordered for the 4-furnace creep test assembly. In these assemblies three specimens can be tested in each furnace. A process control system will be used to control and program each furnace for times up to 1000 hours in both temperature cycling and constant temperature modes. This system should be operable by early 1980.

Plans: The modified creep specimens will be tested in both the dead-weight creep apparatus and the constant strain-rate machine to determine their suitability for use in extended creep tests. Bids for the furnace process control system should be received and started through the procurement system. The anticipated delivery time for the control systems is early 1980; by which time, the assembly of the creep stations should be complete.

* X-317: Mg-Spinel with excess MgO
RFG: Cr-spinel

6. Electrical Transport Mechanisms in Slag Associated with Electrochemical Degradation of Insulator and Electrode Materials, (W. Hosler, T. Negas, and G. White)

Progress:

a. Electrical Conductivity of $YCrO_3$

In order to assess the viability of an electrode material for an MHD generator its physical properties should be investigated. This includes its microstructure and phase composition after material preparation as well as electrical, thermal, and mechanical properties. $LaCrO_3$ doped with either Sr, Ca or Mg has been a leading contender[1] for an electrode and/or lead out material for a hot or semi-hot wall generator. While this material is a good refractory it is also a good conductor even at room temperature. Problems sometimes are encountered, however, due to hydration of the rare earth (La) oxide when the material is either not fully reacted on preparation (or non stoichiometric) or when the transition metal (Cr) evaporates at high temperatures leaving excess La.

Another member of the perovskite family has been developed in this laboratory and at Trans Tech Inc., which is slightly less refractory but has other properties similar to $LaCrO_3$. This material $(YCrO_3)$[2] doped with Ca or Mg does not, however, have the hydration problem associated with the lanthana based perovskites.

The electrical conductivity is dependent on the oxidation state of the chromium. Substitution of a divalent material either on the yttrium or chromium site in the orthorhombic lattice makes it possible to change the chromium valence from +3 in pure $YCrO_3$ to a combination of Cr^{+3} and Cr^{+4} depending on the compensation and oxidation of the material.

Consider the divalent element M^{+2} on the Y site. Then

$$(Y_{1-x}M_x^{+2})(Cr_z^{+4}Cr_{1-z}^{+3})O_{3-\frac{x}{2}+\frac{z}{2}}$$

When z = 0, the material is fully reduced. All chromium is in the +3 state and no electron exchange can take place between Cr^{+3} and Cr^{+4} ions, thus inhibiting hole migration. This results in a low conductivity material as can be seen in the lower curve of Figure 1.

Consider the effect of oxidizing the material to a state such that x = z. No more oxygen can be incorporated into the lattice to preserve charge neutrality and all M^{+2} is compensated for by Cr^{+4} formation. Now electron exchange can take place between Cr^{+4} and Cr^{+3} allowing hole migration and resulting hole conductivity. TEP measurements near room temperature show p type conduction. The upper curve in Figure 1 shows

such a situation for at least partially oxidized $YCrO_3$ doped with Ca on the Y site. Figure 2 shows the same effect for material with Mg on the Y site. The same argument can be made for the dopant placed on the chromium or transition metal site.

$$Y(Cr^{+4}_{z}M^{+3}_{x}Cr^{+3}_{1-x-z})O_{3-\frac{x}{2}+\frac{z}{2}}$$

In the reduced state, as the material is made, z is 0 or very small. All chromium is in the Cr^{+3} state. The divalent ion is charge compensated for by $\frac{x}{2}$ oxygen vacancies (one oxygen vacancy can charge compensate for two M^{+2} substitutions since the valence difference between M^{+2} and Cr^{+3} is only 1). Low conductivity material results. Here again, the conductivity depends on the oxidation state of the material. At higher oxygen pressures z increases allowing some Cr^{+3} to change to Cr^{+4} with resulting electrical conduction. At full oxidation z = x

$$Y(Cr^{+3}_{1-2x}M^{+2}_{x}Cr^{+4}_{x})O_{3}$$

with resulting highest electrical conductivity. The electrical conductivity of the $YCrO_3$ material was measured by the DC four probe technique on samples approximately 3mm square and 25mm long. These samples were contacted with platinum electrodes which were attached by specially prepared platinum material forced into holes drilled in the sample to accept the platinum lead outs. The leads become locked into the holes firmly with resultant zero or undetectable contact resistance. The data was gathered using a Keithley data acquisition system. At each data point, time, TC voltages, current and appropriate voltage drops across the electrodes were recorded and stored in system memory. At the same time, the system was programmed to calculate and print conductivity derived from the current voltage relationship and sample dimensions. The temperature was calculated by the system using stored constants for linearization obtained from NBS Monograph 125, Thermocouple Reference Tables, based on the IPTS-68. All data points shown in Figures 1 and 2 are taken at equilibrium conditions with respect to temperature and oxidation-reduction at high temperatures (>1200 °C) where oxygen diffusion is large. Equilibrium times in this temperature range vary from a few minutes to several hours depending on the temperature and oxygen pressure. Further work is being done on temperature and oxygen pressure dependence of the conductivity.

b. Corrosion of $YCrO_3$ in Slag

Electrochemical corrosion of MHD electrode materials is probably the most severe problem facing the duct portion of the MHD power producing systems. This problem is made more severe when operating at high temperatures. It may be possible however, to offset the disadvantages of accelerated corrosion due to high temperature by the advantages of oper-

ation in the diffuse current mode. Operation at lower temperatures where corrosion is decreased may lead to severe arc damage to the electrode material, thus affecting generator performance. Figure 3 shows a schematic diagram of an electrochemical cell constructed to show the electrochemical degradation of an electrode material when in contact with slag and when carrying current. In an initial experiment, Eastern (Bow, NH) slag was used with 20% K_2SO_4 added to the melt and the electrode material was $YCrO_3$ (.05 Mg). This cell was run for a total time of 16 hours in a constant voltage mode since the purpose of the experiment is to determine the degradation process and electrochemical products formed. The current-time relationship is shown in Figure 5. The $YCrO_3$ electrodes were rectangular prisms 3mm on a side and 10mm long and contacted on the ends not immersed in the slag bath. The temperature was held constant at 1343 °C. Figure 4 is a photograph of a lengthwise cross section of the tested cell. The drop off in current to 20% of the initial value (Figure 5) is most probably due to the build up of a silica rich layer near the anode. This effect had been demonstrated earlier using platinum and $LaCrO_3$ electrodes immersed in coal slag.[3,4] It is obvious that the cathode has been severely attacked but the anode is relatively undamaged. Reaction products at the slag-electrode interfaces have not yet been completely identified. It seems possible however that $YCrO_3$, properly made, may be used as an electrode and/or lead out material dependent on the slag composition and the slag electrode interface temperature. More work will be done on the reaction zone products and temperature effect on electrochemical processes.

c. Slag Electrical Conductivity

A number of measurements have been made on the electrical conductivity of coal slags[5], both natural and synthetic. A question still remains, however, of what specifically is the charge transport mechanism for a given slag at a specific temperature. How much of the conductivity is ionic and how much is electronic? Electrical conductivity measurement on slags is difficult for several reasons. 1. Slags are difficult to hold in any crucible used in a conventional experiment because, when molten, the slag tends to creep out of the vessel thus casting doubt as to the volume content measured; a parameter necessary in the calculation of conductivity values. 2. The chemical state of many components in slag may contribute to the conductivity and this depends on the oxidation or reduction condition which in turn is a function of temperature and, possibly, applied potential. 3. The conductivity can also depend on the phase composition of the slag particularly when solid, *i.e.*, whether the slag is primarily crystalline or glassy or a combination of both. 4. When ionic conductivity is involved, measurement must either be done by AC methods, a difficult and time consuming process because they must be done for each point as a function of frequency, or they may be done by a four probe DC technique providing adequate precautions are taken to eliminate errors due to polarization at the current carrying electrodes. When practical, both methods should be used to complement each other.

We have devised a measuring technique that allows us to eliminate, minimize, or examine these four difficulties. The slag is held in a cylindrical high Al_2O_3 crucible 5cm long and 6mm inside diamter. Pre-cast slag cylinders are placed in the crucible and heated to a temperature in an induction furnace such that the slag is melted and takes the form of the crucible. This procedure prevents slag creep over the crucible walls usually encountered when slag powders and chunks are used in crucible loading. After cooling to room temperature the slag is contacted with four platinum probes carefully spaced along the length of the crucible with the top probe (current) well below ($\geq$ 5mm) the slag surface. This prevents oxidation-reduction conditions from affecting the bulk conductivity values during a measurement as a function of temperature for temperatures where oxygen diffusion is low (solid). A horizontal boat measurement may be in error due to surface oxidation or reduction because the contacts penetrate the exposed surface.

The slag contact is made by drilling a small hole through the crucible wall into the slag and inserting the platinum wire lead-out with a small platinum ball on the end. This wire is then locked into place by specially prepared platinum pressed in the hole around the wire. This method of contacting provides leak free seals for the conductivity probes. The conductivity cell is then placed in a special holder for insertion into the vertical tube furnace for measurement.

One objective is to determine the electrical conductivity of slag and its direct dependence on the ratio of Fe^{+2}/Fe^{+3}. This ratio may be determined by wet chemistry methods which involves the material solution in hydrofluoric and hydrochloric acid in the absence of oxygen and titrating with potassium dichromate. Preliminary measurements indicate that the Fe^{+2} can be determined to a precision of better than $\pm 0.5\%$ by weight. To get the Fe^{+2}/Fe^{+3} ratio, the total iron content must be known. This method promises to give the ratio within 10% accuracy especially in Eastern slags where the iron content is high.

In order to accurately determine the conductivity dependence on the iron oxidation state, the ionic ratio must be maintained constant during the temperature run. To accomplish this the slag was heated to a temperature above its softening or melting point. While holding the temperature constant the conductivity is monitored using the data acquisition system and computer described briefly in section "a" of this task report. When equilibrium is attained (no change in resistance as a function of time) the sample is quenched to a temperature below its melting or softening point where no oxidation or reduction can take place in a reasonable time. Conductivity measurements are then made as a function of temperature below this quench temperature. The Fe^{+2}/Fe^{+3} ratio should be constant.

A new high temperature equilibrium is established with a subsequent quench to low temperature where conductivity measurements are made with

a different Fe^{+2}/Fe^{+3} ratio. The curves shown in Figures 6 and 7 are taken in this manner. Both figures show data for Eastern slag (Bow, NH) without potassium added to the melt. The chemical analysis is given in Table 1.

The dashed portion of the curve represents the conductivity data with increasing temperature which probably reflects the solution of the conducting phase in the high conductivity material into the glassy matrix in the low conductivity material. Many data points were taken in this range (with increasing temperature) but the magnitude in each case depends on the equilibration time or time of solution of the conducting phase Fe_3O_4.

Table 1

Component oxide	Weight %
SiO_2	40.65
Fe_2O_3	20.95
Al_2O_3	22.00
CaO	6.70
K_2O	0.52
Na_2O	0.85
MgO	1.70

The main constituent amounts are typical of an Eastern slag; however, in this analysis they do not add to 100%. Sulfur was found to be about 41 ppm. The component discrepancy is under investigation. Figure 6 is the data taken in an air atmosphere while Figure 7 shows data taken in 5 ppm oxygen in nitrogen. There appears to be little or no oxygen pressure dependence of the conductivity. This slag quenched from a soak temperature about 1375 °C to 900 °C has a conductivity below 900 °C independent of the soak temperature and the conductivity is high. X-ray diffraction measurements show Fe_3O_4 to be a predominant crystalline phase with a slight amount of some other unidentified spinel.

This slag quenched to 900 °C from a temperature below 1375 °C, which is the point at which the slope of the high temperature equilibrium conductivity curve changes, has a conductivity below 900 °C independent of the equilibrium soak temperature below 1375 °C. X-ray diffraction measurements show the only crystalline phase to be anorthite, $CaAl_2Si_2O_8$, a nonconducting material. The conductivity of the slag in this state is low.

The quench times from the soak temperature to 900 °C vary from 22 minutes for a soak temperature of 1510 °C to 15.5 minutes for a soak temperature of 1278 °C. The Fe^{+2}/Fe^{+3} ratios for slag treated under these conditions have not been measured. Scanning electron microscope analysis will be

done in the near future and should give information as to the phase distribution of the iron. The fact that there is a sharp point which is nearly oxygen pressure independent which determines the conductivity state (high or low with nothing intermediate) at low temperature is not completely understood.

Plans: The conductivity of $YCrO_3$ doped with Mg or Ca will be determined carefully as a function of oxygen pressure at several high temperatures. The oxygen pressure will be determined by a zirconia oxygen cell inserted into the sample holder area.

The effect of slag containing potassium on $YCrO_3$ will be determined at several temperatures and the reaction products and damage to the electrodes will be determined by SEM and XRD analysis where possible.

The work on conductivity mechanisms in slag will be continued. Eastern slag containing potassium introduced as potassium sulfate will be investigated as well as, eventually, Western slag (Montana Rosebud) with and without potassium.

Acknowledgements: Special acknowledgements should be given to H. Parker and R. Roth of the Crystal Chemistry section for X-ray diffraction work and helpful discussions on the chemistry of the slag conductivity.

References:

1. Performance of U. S. Electrodes - Insulators Tested in the US-USSR U-02 Phase III Experiment, J. L. Bates and J. L. Daniel, Pacific Northwest Laboratory, Richland, Washington; B. Rossing and J. W. Sadler, Westinghouse Electric Company, Pittsubrgh, Pennsylvania; W. Hosler and T. Negas, National Bureau of Standards - 18th Symposium on Engineering Aspects of MHD, June 18-20, 1979, Butte, Montana.

2. Preparation and Properties of Yttrium Chromite Ceramics, T. Negas, W. Hosler, National Bureau of Standards and L. Dominques, Trans-Tech Inc. 4th International CIMTEC Energy and Ceramic Conference, Faenza, Italy, May 28-31, 1979.

3. Development, Testing and Evaluation of MHD Material, NBS Quarterly Report, October-December 1977, p. 40, DOE Contract No. EA-77-A-01-6010.

4. Electrochemical Corrosion of MHD Electrodes in Coal Slags, L. Cadoff, B. Rossing and H. Smith, 17th Symposium on Engineering Aspects of MHD, Stanford, California, March 27-29, 1978.

5. Open-Cycle Magnetohydrodynamic Electrical Power Generation, Edited by M Petric (USA) and B. Ya Shumyatsky (USSR) - pages 559-567. Argonne National Laboratory, Argonne, Illinois, 1978.

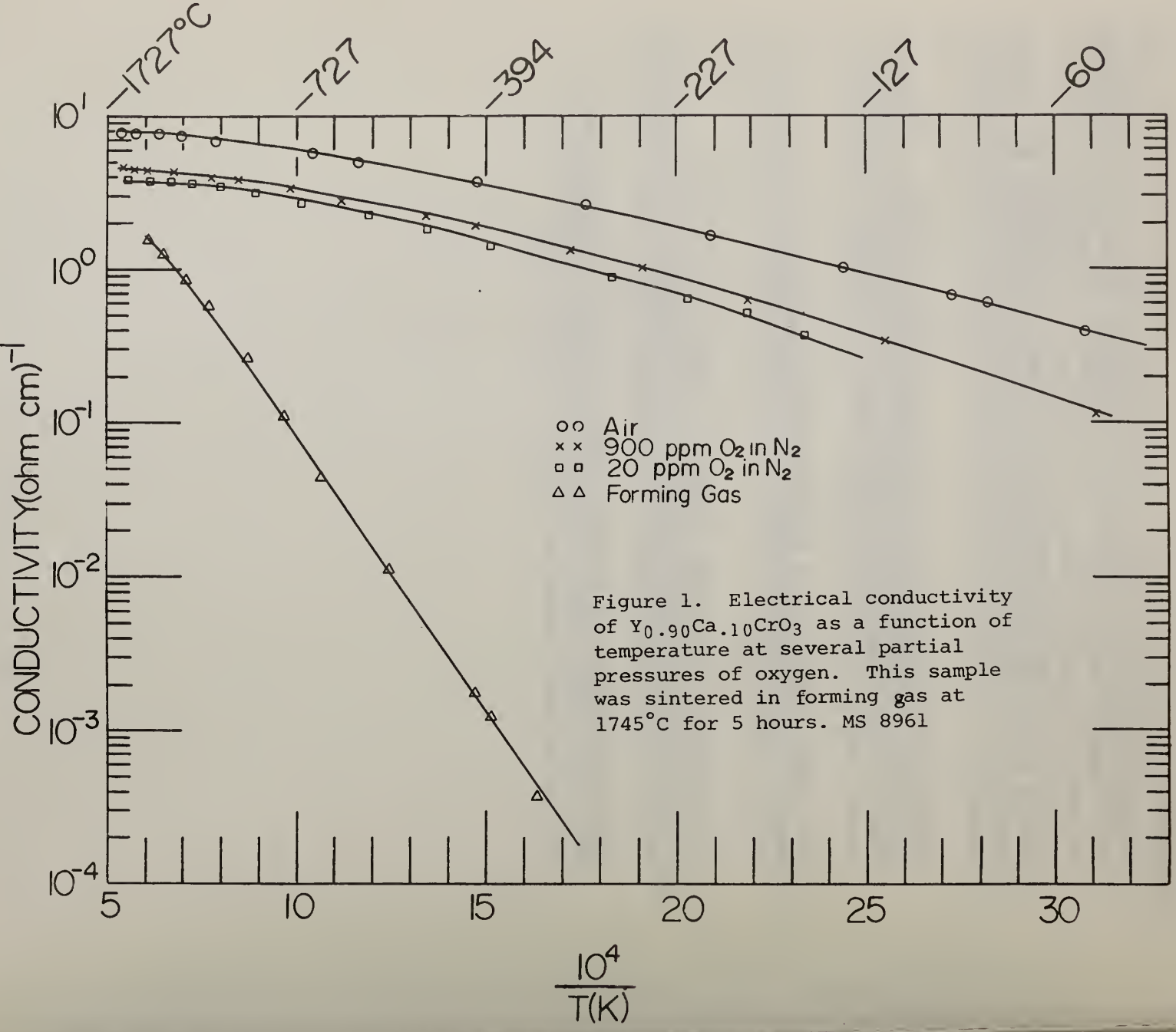

Figure 1. Electrical conductivity of $Y_{0.90}Ca_{.10}CrO_3$ as a function of temperature at several partial pressures of oxygen. This sample was sintered in forming gas at 1745°C for 5 hours. MS 8961

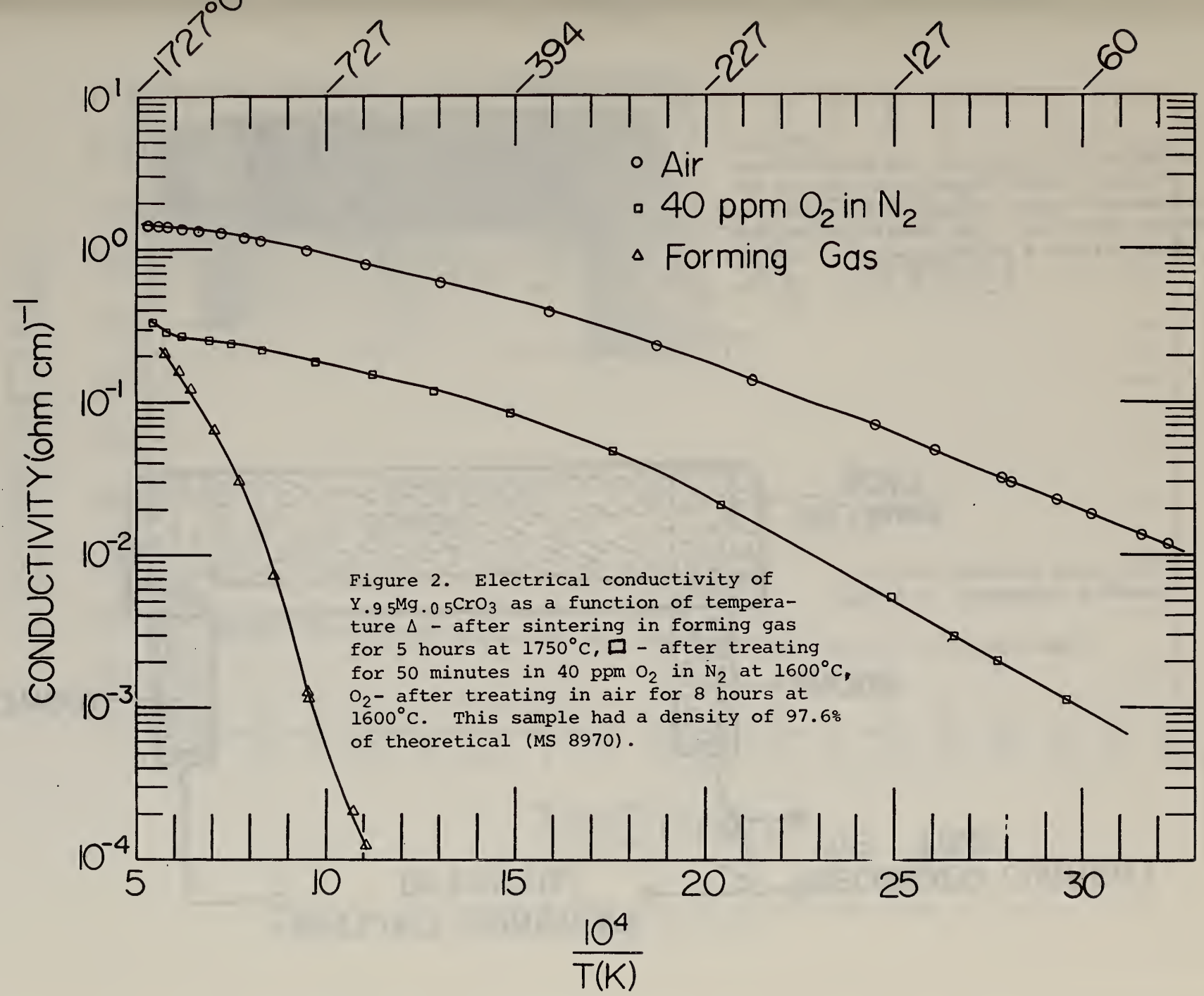

Figure 2. Electrical conductivity of $Y_{.95}Mg_{.05}CrO_3$ as a function of temperature Δ - after sintering in forming gas for 5 hours at 1750°C, □ - after treating for 50 minutes in 40 ppm O_2 in N_2 at 1600°C, O_2- after treating in air for 8 hours at 1600°C. This sample had a density of 97.6% of theoretical (MS 8970).

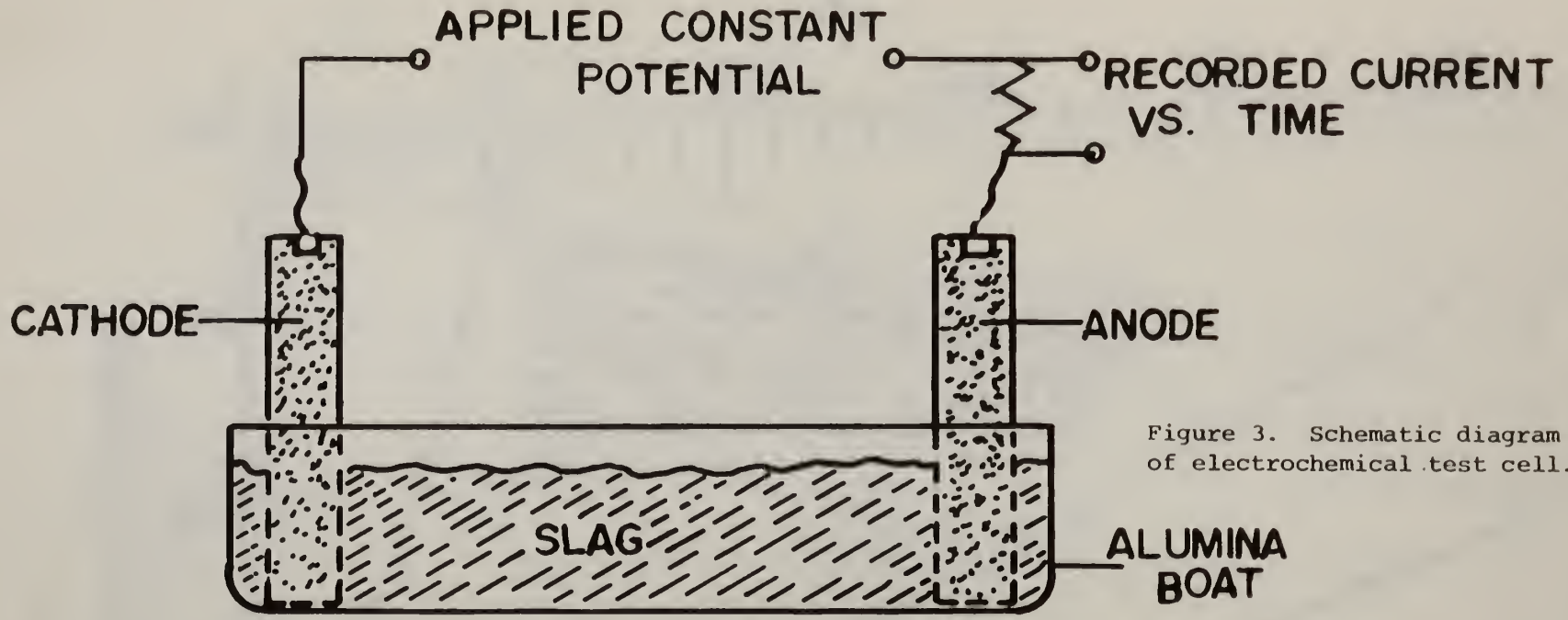

Figure 3. Schematic diagram of electrochemical test cell.

Figure 4. Photograph of a longitudinal section of a test cell. Anode and cathode are $YCrO_3$ with 0.05 Mg fully oxidized to be in high conductivity state. Slag is Eastern (Bow NH) with 20% K_2SO_4 added to the melt.

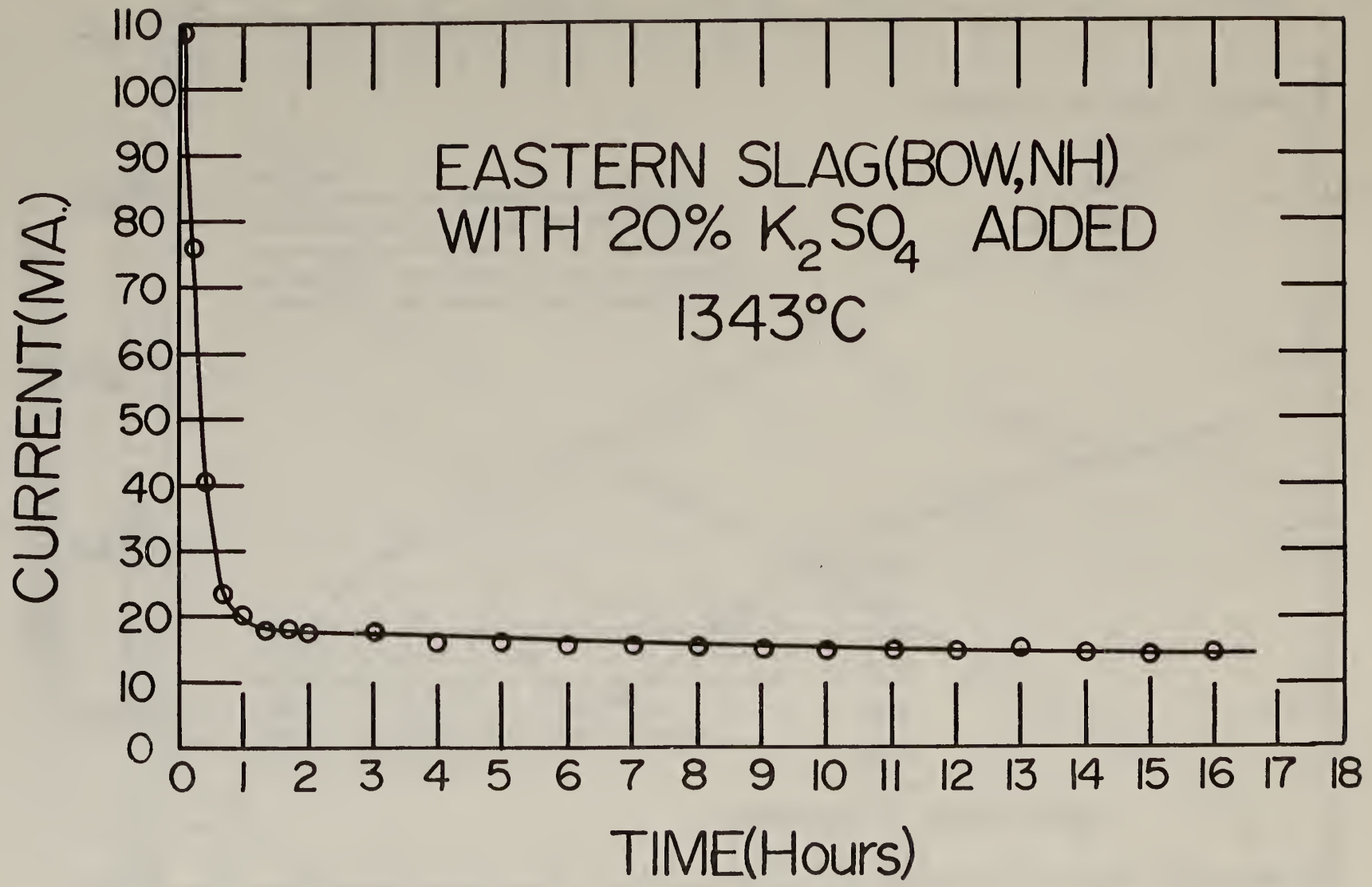

Figure 5. Current-time relationship of the test cell shown in Figure 4. The test temperature was constant at 1343°C.

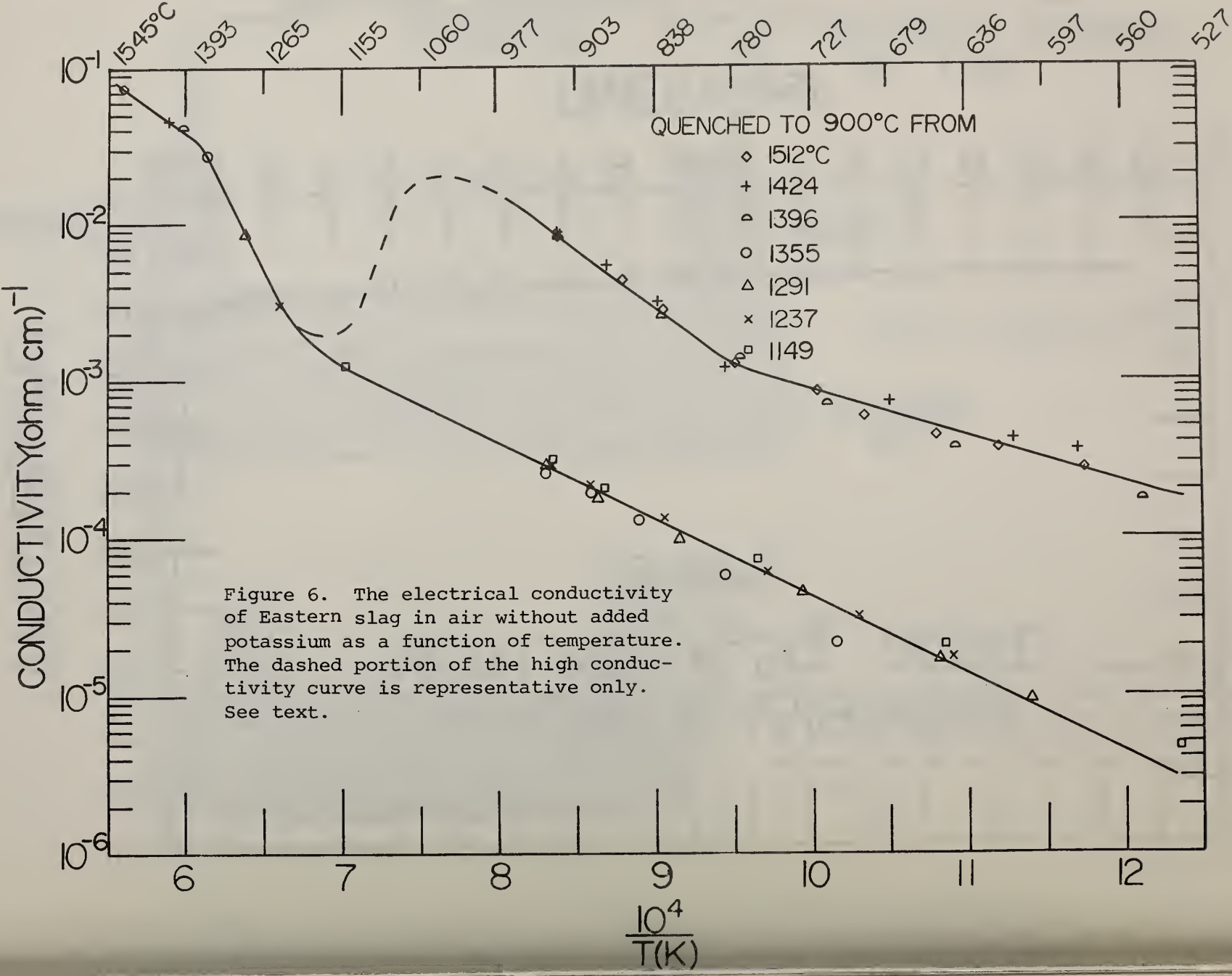

Figure 6. The electrical conductivity of Eastern slag in air without added potassium as a function of temperature. The dashed portion of the high conductivity curve is representative only. See text.

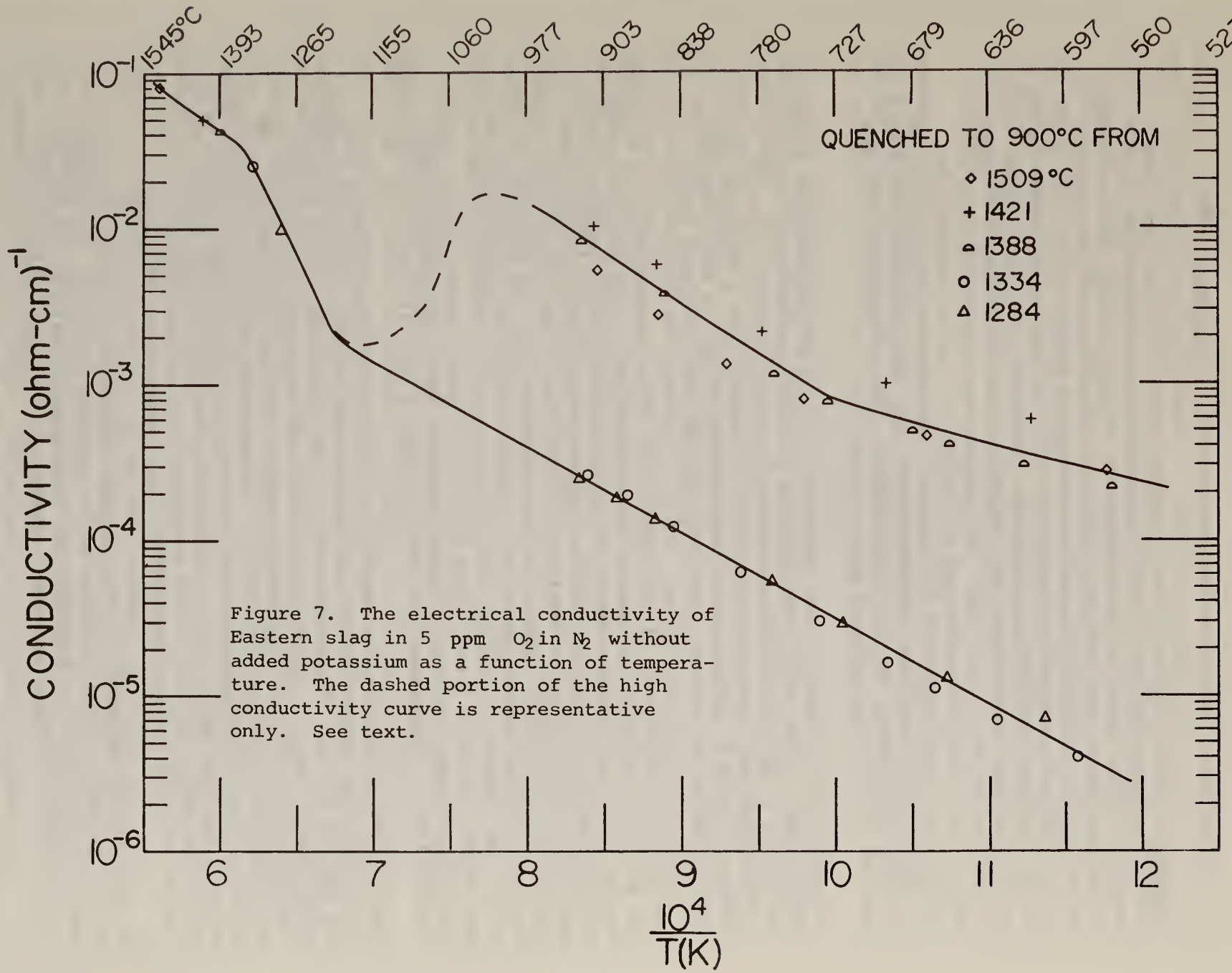

Figure 7. The electrical conductivity of Eastern slag in 5 ppm O_2 in N_2 without added potassium as a function of temperature. The dashed portion of the high conductivity curve is representative only. See text.

7. Corrosion of Downstream MHD Components (J. Smit, 561)

Progress: The objectives of this program are: 1) to develop a test method for assessing the relative corrosion resistance of alloys in downstream components of MHD systems; 2) to screen alloys for corrosion resistance under some simulated downstream conditions; 3) to evaluate the materials subjected to the tests in (2) to determine the conditions under which screened alloys may be suitable candidates for incorporation in the design of downstream components. In order to achieve these objectives, the first sub-task of the program called for extensive changes to be made to an extant test rig. The changes were made to provide more control over test parameters and to extend the testing capabilities of the rig to a longer term ($\geq$ 100 hrs.). To provide this control and to extend operating times, automatic equipment was installed, and a gas handling and storage unit was constructed. The additions and changes detailed below were completed this quarter.

The rebuilt rig, Figure 1, is composed of: 1) a gas handling and storage unit, Figure 2, for oxygen and propane, 2) an instrument unit, Figure 3, containing a two gas blender-controller, a mass flow controller, a thermocouple amplifier unit and digital voltmeters, 3) a vertical test chamber, Figure 4, which houses in descending order: a salt reservoir, burner, combustion chamber, specimen support, and an exhaust duct.

The hot zone temperature of the rebuilt rig is now controlled by a modified two gas blender-controller located between the gas supply and the burner in the oxygen and propane supply lines. This unit, which permits control of both the total flow rate and the oxygen-propane ratio, is interfaced with a thermocouple output amplifier. The output from a monitoring thermocouple (Pt-Pt 10% Rh), which is in close proximity to the specimen in the hot zone, is fed to this amplifier. From the amplifier, the signal goes to the gas blender-controller, which automatically maintains the hot zone gas temperature at a preset fixed value by trimming values in the oxygen and propane lines. During trimming, however, the oxygen-propane ratio remains fixed. Measurements to date indicate a stability of $\pm$10°C at 1200°C.

The specimen temperature is controlled, again automatically, by a mass flow controller located in the cooling air line between the test specimen and the air source. This controller is also interfaced with a thermocouple output amplifier. In operation, the amplifier receives a signal from a thermocouple, Pt-Pt% 10 Rh, which is welded into the test specimen. It amplifies this signal and sends it to the mass controller. The controller maintains the specimen temperature at a preselected value by trimming a valve in the cooling air line. Stability is in the order of $\pm$5°C at 550°C. The thermocouple amplifiers have provisions for voltage read out so that the hot zone and specimen temperatures may be monitored continuously.

The gas storage and handling unit has the capacity to hold six 1-a 220 cu. ft. oxygen cylinders and two 100 lb. propane cylinders. At anticipated flow rates, it is expected that this capacity will be sufficient to allow about seventy-two hours of operation. However, this unit has

been set up with manifolds, control valves and check valves which will permit the removal and replacement of oxygen or propane cylinders without interrupting the supply to the burner. Test duration from this standpoint then is unlimited. All lines in the system, for safety purposes, are metallic, i.e., either copper, stainless steel or heavy walled steel. In addition, again for safety reasons, flash arrestors are located in the oxygen and propane lines just before these gases enter the burner. The piping has been laid out with by-passes so that there is the greatest degree of flexibility for operation. The blender-controller, mass flow controller and flow meters may be bypassed singularly or in combination if necessary or if desired.

Modifications were made to the test chamber itself, Figure 1. Inlet and vents have been placed in the top of the chamber. This allows the front opening to be covered by a sliding, plexiglass window. Easy access to the interior is maintained while improving air flow paths.

One of the test parameters of this program is the oxygen partial pressure near the specimen surface. A Nernst probe is being prepared to make these measurements. The probe, fabricated from a high density zirconia tube, closed on one end, is approximately 0.30 m long and 19 mm in diameter with a wall thickness of approximately 3 mm. An electrode was formed on the exterior of the closed portion of the tube by covering that portion with a platinum gauze and bonding it to that surface with platinum paste. A 0.38 mm platinum lead out wire was spot welded to the gauze prior to bonding. Platinum gauze, to which a 0.38 mm lead out wire was spot welded, was shaped and bonded with platinum paste to the interior of the tube surface directly under the exterior gauze, forming the second electrode. The unit was slowly heated, 2°C/min to 900°C, held for 8 hours and cooled at 2°C/min to room temperature to complete the bonding. Calibration of the Nernst probe will be done in a furnace at varying oxygen partial pressures.

In excess of a dozen specimens of 304 stainless steel, ASTM A 269, have been prepared for test. The specimens are 0.25 m long, 12.7 mm in diameter and have a wall thickness of 0.89 mm. A 0.76 mm diameter hole has been Eloxed in one place at the midpoint of each piece. The hole is the receiver for a Pt-Pt 10% Rh thermocouple which will be welded into place. The specimens have been cleaned according to ASTM G1-72. Three test pieces were cleaned three times according to that schedule and weighed prior to cleaning and after each cleaning to determine weight loss if any through that procedure. The loss was negligible being of the order of 1 to 3 mg for specimens weights around 65.4 grams. This cleaning procedure will also be used in those experiments in which corrosion weight loss determinations will be made.

Plans: In the coming quarter, O_2 partial pressure measurements of the hot gas stream in the vicinity of the specimen will be undertaken, and test specimens of 316 stainless steel, ASTM A 269-75, will be prepared. Four hour and one-hundred hour tests of the 304 stainless steel specimens prepared in this quarter will begin as will some testing of the 316 stainless steel specimens. Evaluation of the tested specimens will be carried out using, singularly or in combination, various metallographic

and analytical techniques. The evaluation will be based on data obtained from corrosion rate (uniform weight loss or wall reduction (mesurements and pit depth measurements and on optical and scanning electron microscopy examinations and on EDX and x-ray diffraction analysis where appropriate.

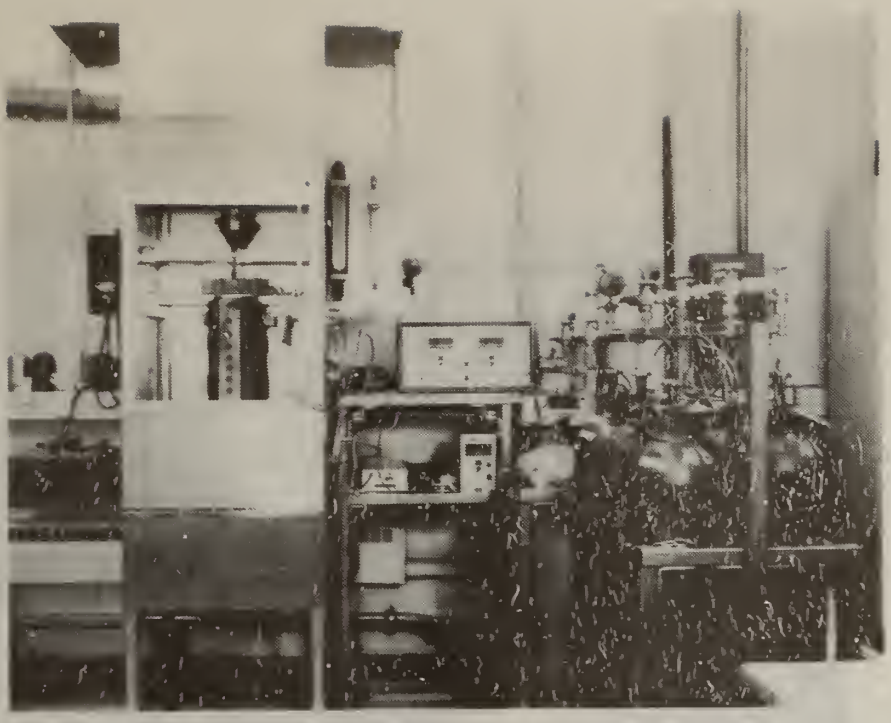

Fig. 1. Test rig showing from left to right the vertical test chamber, an instrument unit and the gas handling and storage unit.

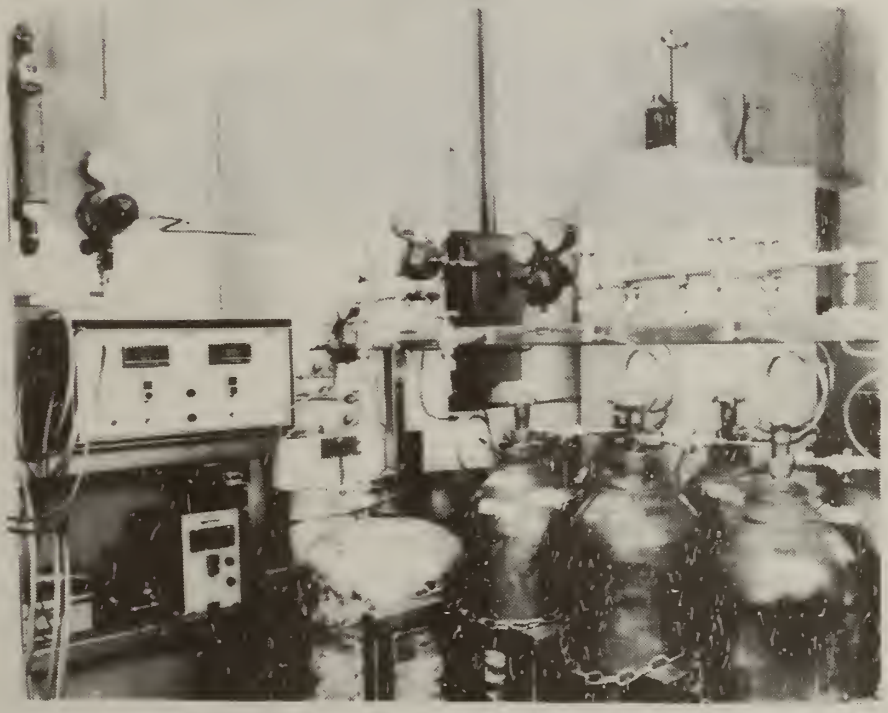

Fig. 2. Gas handling and storage unit.

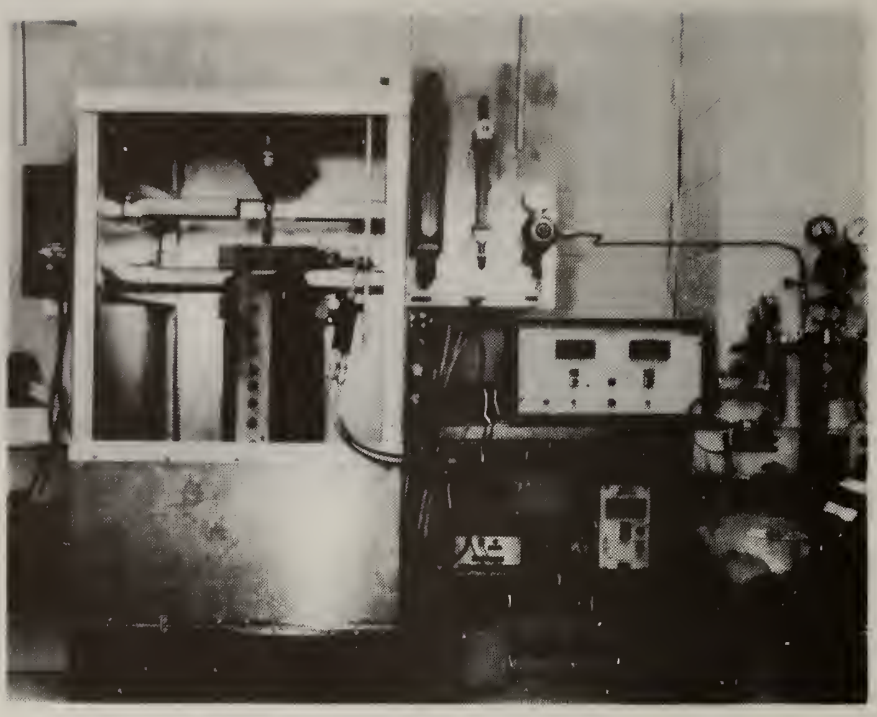

Fig. 3. Instrument unit showing two gas blender controller (large unit center right) and mass flow controller (below blender).

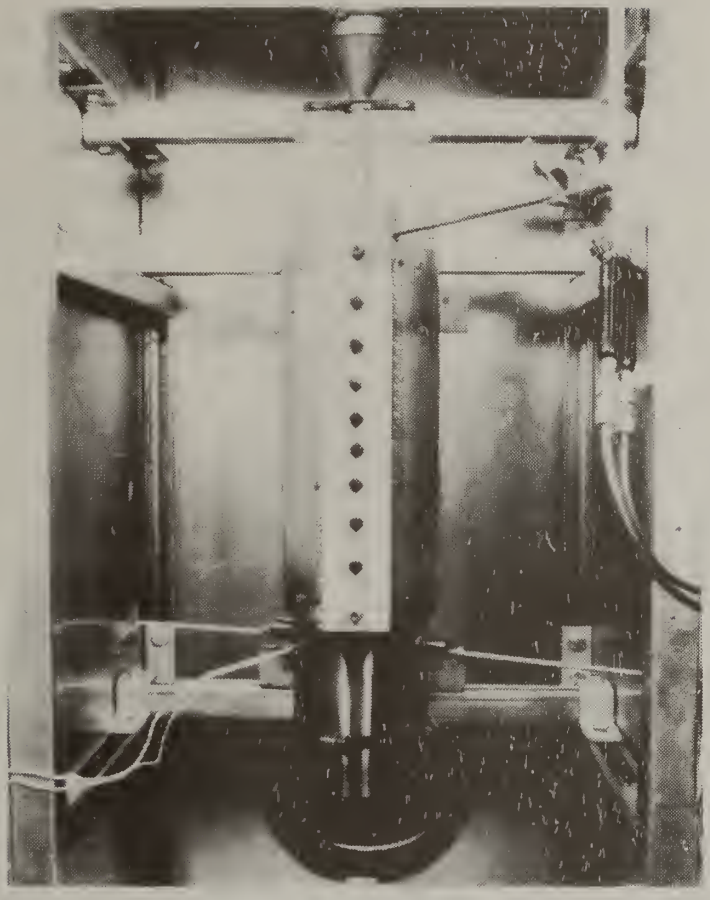

Fig. 4. Vertical test chamber showing from the top salt reservoir burner, combustion chamber and specimen support.